

MOL#86850

Multiple binding sites for small molecule antagonists at the chemokine receptor CCR2

Annelien J.M. Zweemer, Indira Nederpelt, Hilde Vrieling, Sarah Hafith, Maarten L. J. Doornbos, Henk de Vries, Jeffrey Abt, Raymond Gross, Dean Stamos, John Saunders, Martine J. Smit, Adriaan P. IJzerman, Laura H. Heitman

Division of Medicinal Chemistry, Leiden Academic Center for Drug Research, Leiden University, Leiden, The Netherlands (A.J.M., I.N., H.V., S.H., M.L.J.D., H.V., A.P.IJ., L.H.H.); Vertex Pharmaceuticals Inc., San Diego, CA, USA (J.A., R.G., D.S., J.S.); and Division of Medicinal Chemistry, VU University Amsterdam, Amsterdam, The Netherlands (M.J.S.)

MOL#86850

Running title: Multiple binding sites at the chemokine receptor CCR2

Correspondence:

Dr. Laura H. Heitman, Department of Medicinal Chemistry, Leiden Academic Center for

Drug Research, Leiden University, Einsteinweg 55, 2333 CC Leiden, the Netherlands

Phone: +31 (0)71 527 4558, Fax; +31 (0)71 527 4277

E-mail: l.h.heitman@lacdr.leidenuniv.nl

Number of text pages:	40
Number of tables:	4
Number of figures:	8
Number of references:	42
Abstract:	234 words
Introduction:	420 words
Discussion:	1511 words

Abbreviations:

BCA, bicinchoninic acid;

BSA, bovine serum albumin;

CHAPS, 3-((3-cholamidopropyl)-dimethylammonio)-1-propanesulfonate;

CCR2, C-C chemokine receptor 2

CI, Cell Index

EDTA, ethylenediaminetetraacetic acid;

GDP, guanosine diphosphate;

GPCR, G protein-coupled receptor;

MOL#86850

k_{obs} , the observed rate constant to approach equilibrium;

k_{on} , association rate constant;

k_{off} , dissociation rate constant;

NEAA, non-essential amino acids;

PEI, polyethyleneimine;

$t_{1/2}$, dissociation half life

TM, trans-membrane;

U2OS-CCR2: human osteosarcoma cells stably expressing CCR2

MOL#86850

Abstract

The chemokine receptor CCR2 is a G protein-coupled receptor that is primarily activated by the endogenous chemokine CCL2. Many different small molecule antagonists have been developed to inhibit this receptor, as it is involved in a variety of diseases characterized by chronic inflammation. Unfortunately, all of these antagonists lack clinical efficacy and therefore a better understanding of their mechanism of action is warranted. In this study we examined the pharmacological properties of small molecule CCR2 antagonists in radioligand binding and functional assays. Six structurally different antagonists were selected for this study, which all displaced the endogenous agonist ^{125}I -CCL2 from CCR2 with nanomolar affinity. Two of these antagonists, INCB3344 and CCR2-RA, were radiolabeled in order to study the binding site in more detail. We discovered that $[^3\text{H}]$ -INCB3344 and $[^3\text{H}]$ -CCR2-RA bind to distinct binding sites at CCR2, the latter being the first allosteric radioligand for CCR2. Besides the binding properties of the antagonists, we also examined CCR2 inhibition in multiple functional assays, including a novel label-free whole cell assay. INCB3344 was found to competitively inhibit CCL2-induced G protein activation, whereas CCR2-RA showed a non-competitive or allosteric mode of inhibition. These findings demonstrated that the CCR2 antagonists examined in this study can be classified in two groups with a different binding site and thereby a different mode of inhibition. We have provided further insights in CCR2 antagonism, which are important for the development of novel CCR2 inhibitors.

MOL#86850

Introduction

The chemokine receptor CCR2 is a G protein-coupled receptor (GPCR) that can be activated by the endogenous chemokines CCL2, CCL7, CCL8, CCL11 and CCL13. CCR2 is expressed on monocytes, dendritic cells, activated T lymphocytes and basophils and plays an important role in the immune system (Fantuzzi et al., 1999; Jimenez et al.; Luster, 1998). These immune cells migrate to increasing concentrations of chemokines at sites of inflammation as part of the immune response, also known as chemotaxis. Besides this important role in physiology, increased levels of CCR2 and its ligands can induce severe tissue damage. This results in a variety of diseases like multiple sclerosis (Mahad and Ransohoff, 2003), atherosclerosis (Boring et al., 1998), rheumatoid arthritis (Quinones et al., 2005) and neuropathic pain (White et al., 2005), which makes CCR2 an attractive target for the pharmaceutical industry.

Chemokines are thought to bind to their receptors in a two-step manner. First they interact with the extracellular side of the receptor, after which the N-terminus of the chemokine can enter the interhelical binding pocket in the transmembrane (TM) domain in order to activate the receptor (Monteclaro and Charo, 1997; Pease et al., 1998). This binding pocket of chemokine receptors has been divided into a major binding pocket (TM helices 3, 4, 5, 6 and 7) and a minor binding pocket (TM helices 1, 2, 3 and 7) (Surgand et al., 2006). Small molecule antagonists (~600 Da) are at least tenfold smaller than the endogenous chemokines (~8600 Da) and therefore their binding sites can at best only partly overlap. For CCR2 several mutagenesis studies have provided evidence for the binding of small molecule antagonists in the major and minor pocket (Berkhout et al., 2003; Hall et al., 2009; Mirzadegan et al., 2000). These ligands often contain a positively

MOL#86850

charged basic nitrogen that interacts with the conserved negatively charged glutamic acid residue (E291) in TM7, which is directly located between the major and minor binding pocket (Rosenkilde and Schwartz, 2006). In addition several other CCR2 antagonists have been developed that do not possess such a basic nitrogen, and their binding site remains to be elucidated (Struthers and Pasternak, 2010). As there is growing evidence of multiple ligand binding sites for other chemokine receptors, we sought to determine if CCR2 contains several binding sites as well.

To gain a better understanding of the interaction of CCR2 and its ligands, we examined the binding sites and pharmacological properties of six chemically distinct CCR2 antagonists. These antagonists are RS504393 (Mirzadegan et al., 2000), BMS22 (Cherney et al., 2008), Teijin compound 1 (Moree et al., 2008), INCB3344 (Brodmerkel et al., 2005), CCR2-RA-[R] (Bhangoo et al., 2007) and JNJ-27141491 (Buntinx et al., 2008) (Fig. 1). In this study for the first time we provide evidence for two distinct binding sites of small molecule antagonists at the CCR2 receptor. We also discuss the possible biased antagonism of some of the compounds. This work contributes to a better understanding of the nature of the interactions of diverse ligands at the CCR2 receptor.

MOL#86850

Materials and Methods

Chemicals and reagents. CCL2 was purchased from PeproTech (Rocky Hill, NJ) and the CCR2 antagonists BMS22 (Cherney et al., 2008), RS504393 (Mirzadegan et al., 2000) and Teijin compound 1 (Moree et al., 2008) were obtained from Tocris Bioscience (Bristol, UK). INCB3344, JNJ-27141491 and CCR2-RA-[R] were synthesized in-house as described previously (Brodmerkel et al., 2005; Doyon et al., 2008; Xue C, 2004; Zou et al., 2007). [³H]-INCB3344 (specific activity 32 Ci mmol⁻¹) was custom-labeled by Vitrax (Placentia, CA) for which a dehydrogenated precursor of INCB3344 was provided. Notably, INCB3344 was labeled as a racemic mixture of the two isomers *N*-(2-(((3*S*,4*S*)-1-((1*r*,4*S*)-4-(benzo[*d*][1,3]dioxol-5-yl)-4-hydroxycyclohexyl)-4-ethoxypyrrolidin-3-yl)amino)-2-oxoethyl)-3-(trifluoromethyl)benzamide and *N*-(2-(((3*R*,4*R*)-1-((1*r*,4*R*)-4-(benzo[*d*][1,3]dioxol-5-yl)-4-hydroxycyclohexyl)-4-ethoxypyrrolidin-3-yl)amino)-2-oxoethyl)-3-(trifluoromethyl)benzamide, but only the first isomer had sufficient affinity to label CCR2 in our experiments (see below). [³H]-CCR2-RA (specific activity 63 Ci mmol⁻¹) was custom-labeled by Vitrax (Placentia, CA) for which a dehydrogenated precursor of CCR2-RA was provided. CCR2-RA was labeled as a racemic mixture of the two isomers (R)-4-acetyl-1-(4-chloro-2-fluorophenyl)-5-cyclohexyl-3-hydroxy-1,5-dihydro-2H-pyrrol-2-one and (S)-4-acetyl-1-(4-chloro-2-fluorophenyl)-5-cyclohexyl-3-hydroxy-1,5-dihydro-2H-pyrrol-2-one. ¹²⁵I-CCL2 (2200 Ci/mmol) and [³⁵S]-GTPγS (1250 Ci/mmol) were purchased from Perkin-Elmer (Waltham, MA, USA). Bovine serum albumin (BSA, fraction V) was purchased from Sigma (St. Louis, MO, USA). Bicinchoninic acid (BCA) and BCA protein assay reagent were obtained from Pierce Chemical Company (Rockford, IL, USA). Tango™

MOL#86850

CCR2-*bla* U2OS cells stably expressing human CCR2 (U2OS-CCR2) were obtained from Invitrogen (Carlsbad, CA). All other chemicals were obtained from standard commercial sources.

Cell culture. U2OS-CCR2 were cultured in McCoys5a medium supplemented with 10% fetal calf serum, 2 mM glutamine, 0.1 mM non-essential amino acids (NEAA), 25 mM HEPES, 1 mM sodium pyruvate, 100 IU/ml penicillin, 100 µg/ml streptomycin, 100 µg/ml G418, 50 µg/ml hygromycin and 125 µg/ml zeocin in a humidified atmosphere at 37°C and 5% CO₂. Cells were subcultured twice weekly at a ratio of 1:6 on 10 cm ø or 15 cm ø plates by trypsinization.

Cell membrane preparation. Cells were detached from 15 cm ø plates by scraping into 5 ml of phosphate-buffered saline and subsequently centrifuged for 5 min at 3000 rpm. The pellets were resuspended in ice-cold 50 mM Tris-HCl buffer and 5 mM MgCl₂, pH 7.4, and homogenized with an Ultra Turrax homogenizer (IKA-Werke GmbH & Co.KG, Staufen, Germany). Membranes and the cytosolic fraction were separated by centrifugation at 31,000 rpm in an Optima LE-80 K ultracentrifuge (Beckman Coulter, Fullerton, CA) at 4°C for 20 min. The pellet was resuspended in 10 mL of Tris-HCl buffer and the homogenization and centrifugation step were repeated. Finally the membrane pellet was resuspended in 50 mM Tris-HCl buffer and 5 mM MgCl₂, pH 7.4, and aliquots of 250 µL were stored at –80°C. Membrane protein concentrations were measured using a BCA protein determination (Smith et al., 1985).

MOL#86850

¹²⁵I-CCL2 binding assays. Binding assays were performed in a 100 μ L reaction volume containing 50 mM Tris-HCl buffer (pH 7.4), 5 mM MgCl₂, 0.1% 3-((3-cholamidopropyl)-dimethylammonio)-1-propanesulfonate (CHAPS) and 15 μ g of membrane protein at 37°C. For homologous competition experiments, increasing concentrations of CCL2 were incubated with 0.1 nM or 0.05 nM ¹²⁵I-CCL2 for 150 min. At this concentration, total radioligand binding did not exceed 10% of the amount added to prevent ligand depletion. Non specific binding was determined with 10 μ M INCB3344. Displacement assays were performed with 0.1 nM ¹²⁵I-CCL2 using 10 concentrations of competing ligand for 150 min of incubation. Association experiments were performed with 0.1 nM ¹²⁵I-CCL2 at different time intervals of incubation for 3 hrs. Non specific binding was determined for every time point with 10 μ M INCB3344. For dissociation experiments the membranes were first incubated with 0.1 nM ¹²⁵I-CCL2 for 2 hrs. Dissociation was initiated by addition of 10 μ M INCB3344 at different points in time. For all experiments incubations were terminated by dilution with ice-cold 50 mM Tris-HCl buffer supplemented with 0.05% CHAPS and 0.5 M NaCl. Separation of bound from free radioligand was performed by rapid filtration through a 96-well GF/B filter plate pre-coated with 0.25% polyethyleneimine (PEI) using a Perkin Elmer Filtermate-harvester (Perkin Elmer, Groningen, the Netherlands). Filters were washed ten times with ice-cold wash buffer. 25 μ L of Microscint scintillation cocktail (Perkin-Elmer, Groningen, the Netherlands) was added to each well and the filter-bound radioactivity was determined by scintillation spectrometry using the P-E 1450 Microbeta Wallac Trilux scintillation counter (Perkin Elmer, Groningen, The Netherlands).

MOL#86850

[³H]-INCB3344 binding assays. Binding assays were performed in a 100 μ L reaction volume containing 50 mM Tris-HCl buffer (pH 7.4), 5 mM MgCl₂, 0.1% CHAPS and 10 μ g of membrane protein at 25 °C. Saturation experiments were carried out using nine different concentrations of radioligand from 0.5 to 45 nM for 120 min of incubation. Non specific binding was determined at three concentrations of radioligand with 10 μ M BMS22. Displacement assays were carried out with 1.8 nM [³H]-INCB3344 using 10 concentrations of competing ligand for 120 min of incubation. Association experiments were performed with 1.8 nM [³H]-INCB3344 at different time intervals of incubation for 150 min. For dissociation experiments the membranes were first incubated with 1.8 nM [³H]-INCB3344 for 90 min. Dissociation was initiated by addition of 10 μ M of BMS22 at different points in time. In all cases, total radioligand binding did not exceed 10% of the amount added to prevent ligand depletion. For all experiments incubations were terminated by dilution with ice-cold 50 mM Tris-HCl buffer supplemented with 0.05% CHAPS. Separation of bound from free radioligand was performed as described under “¹²⁵I-CCL2 binding assays” using uncoated 96-well GF/B filter plates.

[³H]-CCR2-RA binding assays. Assay conditions were similar as described for [³H]-INCB3344 binding assays. Saturation experiments were carried out using twelve different concentrations of radioligand from 0.1 to 75 nM for 120 min of incubation. Non specific binding was determined at three concentrations of radioligand with 10 μ M JNJ-27141491. Displacement assays were carried out with 3 nM [³H]-CCR2-RA using 6 concentrations of competing ligand for 120 min of incubation. Association experiments were performed with 3 nM [³H]-CCR2-RA at different time intervals of incubation for

MOL#86850

180 min. For dissociation experiments the membranes were first incubated with 3 nM [³H]-CCR2-RA for 90 min. Dissociation was initiated by addition of 10 μM of JNJ-27141491 at different points in time. In all cases, total radioligand binding did not exceed 10% of the amount added to prevent ligand depletion. All experiments were terminated as described under “[³H]-INCB3344 binding assays”.

Tango™ beta-arrestin recruitment assay. The assay was performed using the Tango™ CCR2-*bla* U2OS beta-arrestin recruitment assay kit (Invitrogen, Carlsbad, CA), following the kit protocol. Tango™ CCR2-*bla* U2OS (U2OS-CCR2) cells were cultured in medium supplemented with 10% dialyzed fetal calf serum (Invitrogen, Carlsbad, CA) instead of normal serum for two passages prior to the assay. Briefly, cells were seeded at a density of 40,000 cells per well in Freestyle Expression Medium (Invitrogen, Carlsbad, CA) into a black-wall clear-bottom 96-well plate (Perkin Elmer, MA, USA). Cells were stimulated with increasing concentrations of CCL2 and incubated for 16 hrs at 37°C and 5% CO₂. For antagonist assays, the cells were exposed to increasing concentrations of compound for 30 min prior to stimulation with an EC₈₀ concentration (5 nM) of CCL2 for 16 hrs at 37°C and 5% CO₂. The final DMSO concentration was 0.1% for all assay points. After agonist exposure, the cells were loaded with 16 μL LiveBLAzer FRET B/G substrate for 2 hrs at room temperature. After excitation at 400 nm, fluorescence emission values at 460 nm and 535 nm were measured in an EnVision multilabel plate reader (Perkin Elmer, MA, USA). The ratio of the emission at 460 nm and 535 nm was calculated for each well.

MOL#86850

Label-free whole-cell impedance assay. The xCELLigence RTCA system (Roche Applied Science) was used to perform whole-cell assays (Xi et al., 2008; Yu et al., 2006). TangoTM CCR2-*bla* U2OS (U2OS-CCR2) cells were cultured in medium supplemented with 10% dialyzed fetal calf serum (Invitrogen, Carlsbad, CA) instead of normal serum for two passages prior to the assay. Initially, 50 μ L of culture medium was added to wells in E-plates 96 to obtain background readings followed by the addition of 50 μ L of cell suspension containing 20000 cells per well. The E-plate containing the cells was left at room temperature for 30 min before insertion into the xCELLigence station in the incubator at 37°C and 5% CO₂. The Cell Index (CI) was monitored overnight every 15 min during which cells grew to near confluence. After 16 – 18 hr cells were stimulated with increasing concentrations of CCL2. For the antagonist assays cells were first pre-incubated for 30 min with increasing concentrations of antagonist or vehicle control that was added in 5 μ L compound solution (final concentration of 0.25 % DMSO). Subsequently cells were stimulated with an EC₈₀ concentration (3 nM) of CCL2. Directly after stimulation the measurement frequency was increased to 15-second intervals, followed by 30-second, 1 min and 5 min intervals. For data analysis, the CI values were normalized to CI values prior to ligand addition and baseline corrected with CI traces obtained from vehicle control-treated cells.

[³⁵S]-GTP γ S binding assay. 10 μ g of membranes were diluted in 100 μ L assay buffer containing 50 mM Tris-HCl buffer (pH 7.4), 5 mM MgCl₂, 100 mM NaCl, 1 mM ethylenediaminetetraacetic acid (EDTA), 0.05% BSA, 10 μ M guanosine diphosphate (GDP) and 10 μ g saponin per assaypoint. To determine the IC₅₀ values of antagonists, the

MOL#86850

membranes were pre-incubated with varying concentrations of antagonist for 30 min at 25 °C. Then CCL2 (10 nM) was added followed by another incubation of 30 min and finally the mixture was incubated for 90 min after the addition of [³⁵S]-GTPγS (0.3 nM). To determine the EC₅₀ value of CCL2, the membranes were pre-incubated with varying concentrations of CCL2 in absence (control) or presence of fixed concentrations of antagonist for 30 min at 25 °C. Then [³⁵S]-GTPγS (0.3 nM) was added and the mixture was incubated for 90 min. For all experiments the incubation was terminated by dilution with ice-cold 50 mM Tris-HCl buffer supplemented with 5 mM MgCl₂. Separation of bound from free radioligand was performed as described under “¹²⁵I-CCL2 binding assays” using uncoated 96-well GF/B filter plates.

Data analysis. All experiments were analyzed using the non-linear regression curve fitting program Prism 5 (GraphPad, San Diego, CA, U.S.A.). The K_D values of [³H]-INCB3344 and [³H]-CCR2-RA were obtained by computer analysis of saturation curves according to the equation $\text{bound} = (B_{\text{max}} * [L]) / ([L] + K_d)$ where B_{max} is the maximal number of binding sites (pmol/mg) and K_D is the concentration of radioligand required to reach half-maximal binding. The K_D value of ¹²⁵I-CCL2 was calculated from homologous competition experiments using the Cheng-Prusoff equation, assuming that unlabeled and labeled CCL2 had identical affinities (Cheng and Prusoff, 1973). The dissociation rate constant (*k*_{off}) was obtained by computer analysis of the exponential decay of radioligand binding to the receptor. Association rates were calculated according to the equation $k_{\text{on}} = (k_{\text{obs}} - k_{\text{off}}) / [L]$, where *k*_{obs} was obtained by computer analysis of the exponential association, and [L] is the amount of radioligand used for the association experiments.

MOL#86850

All experiments were fit according to monophasic equations except for dissociation of [³H]-CCR2-RA, which occurred in a biphasic manner. From radioligand displacement data K_i values were calculated from IC_{50} values using the Cheng-Prusoff equation (Cheng and Prusoff, 1973). [³⁵S]-GTP γ S, beta-arrestin recruitment and xCELLigence curves were analyzed by nonlinear regression to obtain IC_{50} or EC_{50} values, where xCELLigence peak responses were obtained within 5 min after compound addition using the RTCA software 1.2 (ACEA Biosciences Inc.). Data shown are the mean \pm S.E.M. of at least 3 separate experiments performed in duplicate. Statistical analysis was performed with a two-tailed unpaired Student's t-test. Comparison of the means of multiple data sets was performed by one-way analysis of variance (ANOVA) followed by a Tukey's multiple comparison test.

MOL#86850

Results

Radioligand binding assays

Characterization of ^{125}I -CCL2. In this study we performed radioligand binding assays for CCR2 with the labeled endogenous agonist ^{125}I -CCL2 as a tracer ligand. To determine the affinity of ^{125}I -CCL2 for CCR2, homologous displacement assays were performed on membranes of U2OS cells stably expressing CCR2 (U2OS-CCR2). This resulted in a K_D of 0.068 ± 0.014 nM and a B_{max} of 0.31 ± 0.03 pmol/mg (Fig. 2A, Table 1). Kinetic association and dissociation experiments were performed to determine the rate constants k_{on} and k_{off} (Fig. 2B). Both the association and dissociation of ^{125}I -CCL2 were best fit by monophasic curves, yielding a k_{on} of 0.29 ± 0.06 nM $^{-1}$ min $^{-1}$ and a k_{off} of 0.033 ± 0.003 min $^{-1}$. The calculated kinetic K_D value ($k_{\text{off}}/k_{\text{on}}$) of 0.12 nM thus agreed fairly well with the affinity obtained in the homologous competition assay.

Displacement of ^{125}I -CCL2 from CCR2. A panel of reference CCR2 antagonists (Fig. 1) was selected for analysis in radioligand displacement assays. U2OS-CCR2 membranes were incubated with ^{125}I -CCL2 and increasing concentrations of antagonist (Fig. 3A). All antagonists fully displaced ^{125}I -CCL2 from the CCR2 receptor with IC_{50} values reported in Table 2. INCB3344 had the highest affinity for CCR2 ($\text{IC}_{50} = 5.4$ nM) followed by BMS22 ($\text{IC}_{50} = 27$ nM), CCR2-RA-[R] ($\text{IC}_{50} = 103$ nM), RS504393 ($\text{IC}_{50} = 132$ nM), JNJ-27141491 ($\text{IC}_{50} = 172$ nM) and Teijin compound 1 ($\text{IC}_{50} = 220$ nM).

The antagonists INCB3344, BMS22, RS504393 and Teijin share structural similarities whereas JNJ-27141491 and CCR2-RA-[R] form a different set of molecules (Fig. 1). We

MOL#86850

decided to tritium-label the two high-affinity compounds INCB3344 and CCR2-RA within the two classes, for which we used two unsaturated precursor molecules that we synthesized in-house. We anticipated that these two molecules would help us in a more detailed characterization of the binding sites of low molecular weight antagonists targeting CCR2.

Characterization of [³H]-INCB3344.

Tritium-labeled INCB3344 is a racemic mixture of two isomers. In ¹²⁵I-CCL2 displacement experiments with the isolated unlabeled isomers we had found that the (3S,4S) isomer had an IC₅₀ of 3.8 ± 0.5 nM, whereas the affinity of the other isomer was at least 1000-fold lower (IC₅₀ = 4.3 ± 0.9 μM). Since we use low nanomolar concentrations (1.8 nM) of [³H]-INCB3344 in the binding studies, we concluded that CCR2 was solely labeled by the high affinity (3S,4S)-isomer.

Saturation binding experiments yielded a K_D of 0.90 ± 0.03 nM with a B_{max} of 7.1 ± 0.2 pmol/mg (Fig 4A, Table 1). Equilibrium binding of [³H]-INCB3344 to U2OS-CCR2 membranes was reached within 1 hour at 25°C as assessed with kinetic association experiments (Fig. 4B). This radioligand was specifically bound to CCR2 as no binding was detected in U2OS membranes that do not express CCR2 (data not shown). Dissociation of [³H]-INCB3344 was initiated by 10 μM of BMS22 and resulted in a t_{1/2} of 53 min at 25°C (Fig. 4B). Both kinetic studies were best fit by monophasic curves, which confirmed that CCR2 was only labeled by one of the isomers. From this data we calculated the association and dissociation rate constants, 0.054 ± 0.002 nM⁻¹ min⁻¹ and

MOL#86850

$0.013 \pm 0.002 \text{ min}^{-1}$ respectively, which resulted in a kinetic K_D of 0.23 nM, in fair agreement with the equilibrium value of 0.90 nM.

Displacement of [³H]-INCB3344 from CCR2. Homologous displacement by INCB3344 yielded a K_i of $1.2 \pm 0.2 \text{ nM}$ (Fig. 3B, Table 2), which corresponded to the K_D that was obtained from saturation binding experiments. CCL2 displaced only 21% of bound [³H]-INCB3344 from the receptor. The antagonists BMS22, RS504393 and Teijin were able to fully displace [³H]-INCB3344 from CCR2 with nanomolar affinities, while JNJ-27141491 and CCR2-RA-[R] did not displace [³H]-INCB3344, which indicates that they bind at a different site at the CCR2 receptor. At a concentration of 1 μM , JNJ-27141491 and CCR2-RA-[R] rather significantly increased [³H]-INCB3344 binding, with 12% and 9% (Student's t-test $p < 0.01$; Table 2), respectively.

Characterization of [³H]-CCR2-RA. CCR2-RA was tritium-labeled as a racemic mixture of two isomers too. In ¹²⁵I-CCL2 displacement experiments the unlabeled (R) and (S) isomers had IC_{50} values of 103 ± 18 and $216 \pm 21 \text{ nM}$, respectively. We can therefore not exclude that CCR2 was labeled to some extent by the lower-affinity isomer too, although we took care to use a low concentration of 3 nM in the displacement assays. Saturation binding experiments yielded a K_D of $5.8 \pm 0.2 \text{ nM}$ with a B_{max} of $9.7 \pm 0.2 \text{ pmol/mg}$ (Fig 5A, Table 1). Equilibrium binding of [³H]-CCR2-RA to U2OS-CCR2 membranes was reached within 2 hours at 25°C as assessed with kinetic association experiments following a monophasic fit (Fig. 5B). This radioligand was specifically bound to CCR2 as no binding was detected in U2OS membranes that do not express

MOL#86850

CCR2 (data not shown). Dissociation of [³H]-CCR2-RA was initiated by 10 μM of JNJ-27141491 and resulted in a biphasic dissociation pattern with k_{off1} and k_{off2} of $0.24 \pm 0.02 \text{ min}^{-1}$ and $0.029 \pm 0.005 \text{ min}^{-1}$, respectively (Fig. 5C).

Displacement of [³H]-CCR2-RA from CCR2. CCL2 displaced only 23% of bound [³H]-CCR2-RA from the receptor (Fig. 3C, Table 2). The antagonists JNJ-27141491 and CCR2-RA-[R] were able to fully displace [³H]-CCR2-RA from CCR2 with nanomolar affinities, while antagonists INCB3344, BMS22, RS504393 and Teijin did not displace [³H]-CCR2-RA, suggesting that they bind at a different site at the CCR2 receptor. In contrast, INCB3344, BMS22, RS504393 and Teijin significantly increased [³H]-CCR2-RA binding with 69%, 64%, 57% and 59% at a concentration of 1 μM, respectively (Student's t-test $p < 0.05$; Table 2).

Functional assays

In addition to radioligand binding experiments we also performed a number of functional assays, both G protein-dependent and –independent.

Inhibition of beta-arrestin recruitment to CCR2. We first performed beta-arrestin recruitment assays (G protein-independent) to assess the inhibitory potency of all six antagonists. CCL2 induced beta-arrestin recruitment to CCR2 with an EC_{50} of $1.4 \pm 0.4 \text{ nM}$ ($n=4$) (Fig. 6A). All antagonists were able to inhibit beta-arrestin recruitment induced by 5 nM CCL2 (Fig. 6B, Table 3). Interestingly, JNJ-27141491 and CCR2-RA-[R] were more potent inhibitors of beta-arrestin recruitment than Teijin and RS504393, while these antagonists showed equal affinities in the ¹²⁵I-CCL2 displacement assay.

MOL#86850

Analysis of CCR2 inhibition in an impedance-based label-free whole-cell assay. The xCELLigence RTCA system was used to study the activation and inhibition of CCR2 in a label-free whole-cell assay. Typically, addition of CCL2 resulted in an immediate dose dependent increase in Cell Index (CI) to a peak level within 5 min, followed by a second peak after approximately 20 min, which then returned to baseline after one hour of incubation (Fig. 7A). Concentration-effect curves were obtained by analysis of the peak-level that appeared within 5 min after stimulation and resulted in an EC_{50} value of 1.1 ± 0.1 nM for CCL2 (n=5) (Fig. 7B). Pre-incubation with all antagonists resulted in an inhibition of the CCL2-induced response (Fig. 7C, Table 3). The antagonists were equally potent to inhibit CCL2-induced impedance effects as they were able to inhibit beta-arrestin recruitment, except for Teijin and CCR2-RA-[R], which were less potent to inhibit the impedance response with IC_{50} values of 292 ± 66 nM and 64 ± 14 nM, respectively.

[35 S]-GTP γ S binding to CCR2. We also performed a G protein-dependent functional assay. For this purpose, we used a [35 S]-GTP γ S binding assay on U2OS-CCR2 membranes, where we measured G protein activation by CCL2 in absence or presence of different antagonists (Fig. 8). CCL2 stimulated [35 S]-GTP γ S binding with an EC_{50} value of 5.7 ± 0.9 nM (n=8, see also Fig. 8B and 8C). All antagonists were able to inhibit CCL2-induced G protein activation (Fig. 8A, Table 3). Notably, RS504393 and JNJ-27141491 were more potent inhibitors of G protein activation than of beta-arrestin

MOL#86850

recruitment or the impedance response evoked by CCL2, their IC_{50} values being 19 ± 7 nM and 3.9 ± 1.0 nM, respectively.

Based on the displacement data obtained with [3 H]-INCB3344 and [3 H]-CCR2-RA, INCB3344 and CCR2-RA-[R] were selected as representative antagonists for the two putative distinct binding sites. To examine their mechanism of inhibition in more detail, we analyzed the shift of CCL2-induced [35 S]-GTP γ S binding in the presence of fixed concentrations of antagonist. The maximal effect of CCL2 in the presence of CCR2-RA-[R] was significantly reduced, while CCL2's potency was slightly, but similarly decreased at all three antagonist concentrations (Fig. 8C; Table 4). In contrast, the addition of INCB3344 markedly decreased the EC_{50} value of CCL2, while the efficacy of CCL2 was unaffected (Fig. 8B; Table 4). A Schild-plot analysis of the INCB3344 data yielded a K_B value of 0.4 nM, which is in close agreement with the K_D value of 0.9 nM determined in the saturation binding assay. Overall, these data indicate that INCB3344 behaved as a competitive antagonist, whereas CCR2-RA-[R] clearly showed non-competitive antagonism for CCR2 with respect to CCL2, as indicated by a decrease in CCL2's efficacy in the presence of increasing concentrations of CCR2-RA-[R].

MOL#86850

Discussion

Previous studies reported CCR2 and its endogenous ligand CCL2 as major players in a variety of diseases (Boring et al., 1998; Mahad and Ransohoff, 2003; White et al., 2005). Given this potential role as a drug target, the pharmaceutical industry has developed many CCR2 antagonists, (Struthers and Pasternak, 2010), although without much clinical success. Given the variety in chemical scaffolds it is surprising that little attention, if at all, has been paid to the binding mode of these ligands to the receptor. Therefore, the present study was designed to compare the binding site and mechanism of inhibition for a selection of these antagonists.

To study the binding of these antagonists to CCR2 we used the radioligand ^{125}I -CCL2 and the custom-labeled small molecule radioligands [^3H]-INCB3344 and [^3H]-CCR2-RA. We found an affinity constant of 0.068 nM for ^{125}I -CCL2, which corresponds to reported data in literature (K_D 0.05 nM (Samson et al., 1997; Springael et al., 2006)). In addition, the dissociation rate constant of ^{125}I -CCL2 from U2OS-CCR2 membranes of 0.033 min^{-1} is in agreement with the previously reported k_{off} of 0.036 min^{-1} (Springael et al., 2006). [^3H]-INCB3344 was previously published and characterized as a radioligand for CCR2 (Shin et al., 2009). In those studies a K_D value of 5 nM was reported for HEK293 cells stably expressing CCR2. Our experiments with U2OS-CCR2 cells resulted in a 5-fold lower K_D value of 0.9 nM. This difference could be the result of the different cell type, different assay buffer, or the longer incubation time that was used in our assay.

In this study [^3H]-CCR2-RA is reported as the first allosteric radioligand for CCR2. It was characterized as a high affinity radioligand ($K_D = 5.8 \text{ nM}$) that reversibly binds to the receptor. The biphasic dissociation of [^3H]-CCR2-RA from CCR2 could be a result of the

MOL#86850

racemic nature of the radioligand. The B_{\max} for [^3H]-CCR2-RA and [^3H]-INCB3344 were 31-fold and 23-fold higher than for ^{125}I -CCL2. A possible explanation might be that part of the receptors present in vesicular structures in the membrane preparations are only accessible to membrane permeable molecules, such as CCR2-RA and INCB3344, but not to CCL2. In addition, allosteric interactions described within chemokine receptor oligomers might modify the apparent number of binding sites for some radioligands (El-Asmar et al., 2005; Sohy et al., 2007). Finally, antagonists like CCR2-RA and INCB3344 supposedly bind to the G protein-coupled state as well as the uncoupled state of the receptor, whereas the agonist CCL2 presumably only binds to the G protein-coupled state (i.e. labeling a smaller population of receptors). This was confirmed by experiments in the presence of GTP, which uncouples the receptor from its G protein, since these resulted in a complete loss of binding of ^{125}I -CCL2, while binding of [^3H]-INCB3344 and [^3H]-CCR2-RA was not affected (data not shown). Similar extensive differences in B_{\max} values between radiolabeled agonist and antagonist have previously been reported for the CXCR2 chemokine receptor (de Kruijf et al., 2009). In any case, the three radioligands do not label the same receptor populations. This may therefore contribute to the different IC_{50} values derived from competition experiments performed with either CCL2 or a small molecule as a radioligand.

INCB3344 and CCR2-RA-[R] were able to fully displace ^{125}I -CCL2 receptor binding, while CCL2 was only capable of displacing 21% of [^3H]-INCB3344 binding and 19% of [^3H]-CCR2-RA binding. This could be explained by the heterogeneity of binding sites and the G protein uncoupling of a fraction of CCR2. In addition, the incomplete displacement could suggest that CCL2, INCB3344 and CCR2-RA bind to different sites

MOL#86850

at CCR2. Given the size of INCB3344 (578 Da) and CCR2-RA (352 Da) these ligands can at best only partly overlap with the binding site of the large peptide CCL2 (8600 Da). The three different radioligands were used to study and compare six structurally different CCR2 antagonists. All antagonists displaced ^{125}I -CCL2 from the receptor (Fig. 3A, Table 2) with affinities that are similar to previously reported data (Brodmerkel et al., 2005; Buntinx et al., 2008; Cherney et al., 2008; Mirzadegan et al., 2000; Moree et al., 2008; Zou et al., 2007). BMS22, RS504393 and Teijin were also able to displace [^3H]-INCB3344 binding, which indicated that these four ligands share a common binding site. On the contrary, JNJ-27141491 and CCR2-RA-[R] did not displace [^3H]-INCB3344 from CCR2 (Fig. 3B). Analogous results were found in the [^3H]-CCR2-RA displacement assay, where INCB3344, BMS22, RS504393 and Teijin did not displace [^3H]-CCR2-RA from CCR2 (Fig. 3C). Therefore we conclude that there are at least two different binding sites for small molecule antagonists at CCR2. Notably, at high concentrations JNJ-27141491 and CCR2-RA-[R] significantly increased [^3H]-INCB3344 binding to CCR2, whereas INCB3344, BMS22, RS504393 and Teijin significantly increased [^3H]-CCR2-RA binding to CCR2 (Table 2). This behavior is indicative for allosteric enhancement, best explained by the two compounds stabilizing the same conformation of the receptor by binding at two topographically different sites (Lazareno and Birdsall, 1995).

For RS504393, Teijin and BMS22 mutagenesis studies have shown that these molecules bind to the major and/or minor binding pocket of CCR2. RS504393 and Teijin interact with the highly conserved glutamic acid residue E291 most likely via their basic nitrogen atom (Hall et al., 2009; Mirzadegan et al., 2000). For BMS22, the adjacent T292 was found to be important for binding (Cherney et al., 2008), indicating that it shares the same

MOL#86850

binding pocket as RS504393 and Teijin. Notably, for INCB3344 no such data has been reported yet and here we established that it binds to the same site as RS504393, Teijin and BMS22. The presence of a basic nitrogen in the pyrrolidine ring of INCB3344 suggests a similar interaction with E291.

The structures of JNJ-27141491 and CCR2-RA-[R] contain different chemical features in comparison to the other antagonists. JNJ-27141491 and CCR2-RA-[R] lack a basic nitrogen, have a lower molecular weight and are acidic in nature. Their exact binding site or sites at CCR2 remain to be determined. For several other chemokine receptors the presence of an allosteric binding site has been reported (Scholten et al., 2011). Whereas some antagonists interact with both the major and minor binding pocket in the transmembrane region, others bind exclusively to either one of these sites. Given the large size of this binding pocket, the two different binding sites that we have identified for CCR2 could both be located in this transmembrane region. In addition, an allosteric binding site on the intracellular side of the receptor in the C-terminal domain has been identified for the chemokine receptors CXCR2, CCR4 and CCR5 (Andrews et al., 2008; Nicholls et al., 2008; Salchow et al., 2010). This binding site resides close to the site of G protein coupling to the receptor and therefore it is assumed that activation of the G protein is prevented in the presence of an antagonist at this site. The intracellular antagonists of CXCR2 contain an acidic centre (Salchow et al., 2010), which is also present in JNJ-27141491 and CCR2-RA-[R]. In addition, CCR2 and CCR5 are closely related based on sequence similarity. Hence, the presence of such an intracellular binding site for CCR2 is not unlikely.

MOL#86850

By means of functional assays we confirmed that the six compounds described in this paper are indeed CCR2 antagonists, at the G protein level, in beta-arrestin recruitment and in a novel label-free impedance-based functional assay (Table 3). Analysis of these differential functional responses allowed us to explore if these ligands show biased antagonism, which has been described for allosteric ligands of other GPCRs (Kenakin and Miller, 2010; Magnan et al., 2013). Notably, it has been reported that some CCR2 antagonists are capable of discriminating between different functional states of the receptor (Kredel et al., 2011). In our hands RS504393 and JNJ-27141491 were slightly more potent inhibitors of G protein activation, whereas Teijin was most potent in the beta-arrestin recruitment assay. Except for these small but significant differences, all antagonists were equally potent amongst the different functional assays, and as such there is little indication of biased antagonism in our assays. As the effect in functional assays is dependent on the off-rate of the antagonists, which are at present unknown, we do realize that it is difficult to compare the three functional assays as their incubation times varies from minutes to hours.

We next determined the mechanism of inhibition in a [³⁵S]-GTPγS assay for INCB3344 and CCR2-RA-[R] as representative compounds binding to different binding sites. INCB3344 behaved as a competitive antagonist, whereas CCR2-RA-[R] showed noncompetitive antagonism for CCR2 with respect to CCL2 (Fig. 7). Agonist stimulation after pre-incubation with an antagonist can result in submaximal receptor stimulation if the antagonist is not sufficiently dissociated to liberate the entire population at the time at which the maximal response is measured (Vauquelin et al., 2002). Therefore we co-incubated increasing concentrations of CCL2 in presence of fixed amounts of antagonist

MOL#86850

to rule out insurmountable antagonism due to slow dissociation kinetics. The mechanism of INCB3344 inhibition was previously addressed in a calcium flux assay in human monocytes and a competition binding assay using ^{125}I -CCL2 (Shin et al., 2009). Both experiments showed a competitive mode of inhibition with respect to CCL2. These results are in good agreement with our competitive profile of INCB3344 in the [^{35}S]-GTP γ S assay.

For CCR2-RA-[R] no detailed pharmacological data was previously published, except for its inhibition of pain behavior in an *in vivo* model with nerve-injured rats (Bhangoo et al., 2007). We now provide evidence for a noncompetitive mode of inhibition of CCR2. Based on the results of our binding studies we assume that CCR2-RA-[R] and JNJ-27141491 bind to a similar site at CCR2, or at least bind to a site that is distinct from INCB3344's binding pocket. Since JNJ-27141491 was previously published as a noncompetitive antagonist of CCR2, it is therefore very likely that CCR2-RA-[R] and JNJ-27141491 bind and inhibit CCR2 via a similar mechanism (Buntinx et al., 2008).

In summary, we have demonstrated that the CCR2 antagonists examined in this study can be classified into at least two groups with a different binding site and thereby a different mode of inhibition. Hence we have provided further insights into CCR2 antagonism, which may be relevant for the development of novel CCR2 inhibitors.

MOL#86850

Authorship contributions

Participated in research design: Zweemer, Smit, Stamos, Saunders, IJzerman, Heitman.

Conducted experiments: Zweemer, Nederpelt, Doornbos, Hafith, de Vries, Vrieling.

Contributed new reagents or analytic tools: Abt, Gross.

Performed data analysis: Zweemer, Nederpelt, Doornbos, Hafith, de Vries, Vrieling.

Wrote or contributed to the writing of the manuscript: Zweemer, Smit, IJzerman,

Heitman

MOL#86850

References

- Andrews G, Jones C and Wreggett KA (2008) An intracellular allosteric site for a specific class of antagonists of the CC chemokine G protein-coupled receptors CCR4 and CCR5. *Mol Pharmacol* **73**(3):855-867.
- Berkhout TA, Blaney FE, Bridges AM, Cooper DG, Forbes IT, Gribble AD, Groot PH, Hardy A, Ife RJ, Kaur R, Moores KE, Shillito H, Willetts J and Witherington J (2003) CCR2: characterization of the antagonist binding site from a combined receptor modeling/mutagenesis approach. *J Med Chem* **46**(19):4070-4086.
- Bhangoo S, Ren D, Miller RJ, Henry KJ, Lineswala J, Hamdouchi C, Li B, Monahan PE, Chan DM, Ripsch MS and White FA (2007) Delayed functional expression of neuronal chemokine receptors following focal nerve demyelination in the rat: a mechanism for the development of chronic sensitization of peripheral nociceptors. *Mol Pain* **3**:38.
- Boring L, Gosling J, Cleary M and Charo IF (1998) Decreased lesion formation in CCR2^{-/-} mice reveals a role for chemokines in the initiation of atherosclerosis. *Nature* **394**(6696):894-897.
- Brodmerkel CM, Huber R, Covington M, Diamond S, Hall L, Collins R, Leffet L, Gallagher K, Feldman P, Collier P, Stow M, Gu X, Baribaud F, Shin N, Thomas B, Burn T, Hollis G, Yeleswaram S, Solomon K, Friedman S, Wang A, Xue CB, Newton RC, Scherle P and Vaddi K (2005) Discovery and pharmacological characterization of a novel rodent-active CCR2 antagonist, INCB3344. *J Immunol* **175**(8):5370-5378.
- Buntinx M, Hermans B, Goossens J, Moechars D, Gilissen RA, Doyon J, Boeckx S, Coesemans E, Van Lommen G and Van Wauwe JP (2008) Pharmacological profile of JNJ-27141491 [(S)-3-[3,4-difluorophenyl]-propyl]-5-isoxazol-5-yl-2-thioxo-2,3-dihydro-1H-imidazole-4-carboxyl acid methyl ester], as a noncompetitive and orally active antagonist of the human chemokine receptor CCR2. *J Pharmacol Exp Ther* **327**(1):1-9.
- Cheng Y and Prusoff WH (1973) Relationship between the inhibition constant (K₁) and the concentration of inhibitor which causes 50 per cent inhibition (I₅₀) of an enzymatic reaction. *Biochem Pharmacol* **22**(23):3099-3108.
- Cherney RJ, Mo R, Meyer DT, Nelson DJ, Lo YC, Yang G, Scherle PA, Mandlekar S, Wasserman ZR, Jezak H, Solomon KA, Tebben AJ, Carter PH and Decicco CP (2008) Discovery of disubstituted cyclohexanes as a new class of CC chemokine receptor 2 antagonists. *J Med Chem* **51**(4):721-724.
- de Kruijf P, van Heteren J, Lim HD, Conti PG, van der Lee MM, Bosch L, Ho KK, Auld D, Ohlmeyer M, Smit MJ, Wijkmans JC, Zaman GJ and Leurs R (2009) Nonpeptidergic allosteric antagonists differentially bind to the CXCR2 chemokine receptor. *J Pharmacol Exp Ther* **329**(2):783-790.
- Doyon J, Coesemans E, Boeckx S, Buntinx M, Hermans B, Van Wauwe JP, Gilissen RA, De Groot AH, Corens D and Van Lommen G (2008) Discovery of potent, orally bioavailable small-molecule inhibitors of the human CCR2 receptor. *ChemMedChem* **3**(4):660-669.

MOL#86850

- El-Asmar L, Springael JY, Ballet S, Andrieu EU, Vassart G and Parmentier M (2005) Evidence for negative binding cooperativity within CCR5-CCR2b heterodimers. *Mol Pharmacol* **67**(2):460-469.
- Fantuzzi L, Borghi P, Ciolli V, Pavlakis G, Belardelli F and Gessani S (1999) Loss of CCR2 expression and functional response to monocyte chemotactic protein (MCP-1) during the differentiation of human monocytes: role of secreted MCP-1 in the regulation of the chemotactic response. *Blood* **94**(3):875-883.
- Hall SE, Mao A, Nicolaidou V, Finelli M, Wise EL, Nedjai B, Kanjanapangka J, Harirchian P, Chen D, Selchau V, Ribeiro S, Schyler S, Pease JE, Horuk R and Vaidehi N (2009) Elucidation of binding sites of dual antagonists in the human chemokine receptors CCR2 and CCR5. *Mol Pharmacol* **75**(6):1325-1336.
- Jimenez F, Quinones MP, Martinez HG, Estrada CA, Clark K, Garavito E, Ibarra J, Melby PC and Ahuja SS CCR2 plays a critical role in dendritic cell maturation: possible role of CCL2 and NF-kappa B. *J Immunol* **184**(10):5571-5581.
- Kenakin T and Miller LJ (2010) Seven transmembrane receptors as shapeshifting proteins: the impact of allosteric modulation and functional selectivity on new drug discovery. *Pharmacol Rev* **62**(2):265-304.
- Kredel S, Wolff M, Hobbie S, Bieler M, Gierschik P and Heilker R (2011) High-content analysis of CCR2 antagonists on human primary monocytes. *J Biomol Screen* **16**(7):683-693.
- Lazareno S and Birdsall NJ (1995) Detection, quantitation, and verification of allosteric interactions of agents with labeled and unlabeled ligands at G protein-coupled receptors: interactions of strychnine and acetylcholine at muscarinic receptors. *Mol Pharmacol* **48**(2):362-378.
- Luster AD (1998) Chemokines--chemotactic cytokines that mediate inflammation. *N Engl J Med* **338**(7):436-445.
- Magnan R, Escrieut C, Gigoux V, De K, Clerc P, Niu F, Azema J, Masri B, Cordomi A, Baltas M, Tikhonova IG and Fourmy D (2013) Distinct CCK-2 receptor conformations associated with beta-arrestin-2 recruitment or phospholipase-C activation revealed by a biased antagonist. *J Am Chem Soc* **135**(7):2560-2573.
- Mahad DJ and Ransohoff RM (2003) The role of MCP-1 (CCL2) and CCR2 in multiple sclerosis and experimental autoimmune encephalomyelitis (EAE). *Semin Immunol* **15**(1):23-32.
- Mirzadegan T, Diehl F, Ebi B, Bhakta S, Polsky I, McCarley D, Mulkins M, Weatherhead GS, Lapierre JM, Dankwardt J, Morgans D, Jr., Wilhelm R and Jarnagin K (2000) Identification of the binding site for a novel class of CCR2b chemokine receptor antagonists: binding to a common chemokine receptor motif within the helical bundle. *J Biol Chem* **275**(33):25562-25571.
- Monteclaro FS and Charo IF (1997) The amino-terminal domain of CCR2 is both necessary and sufficient for high affinity binding of monocyte chemoattractant protein 1. Receptor activation by a pseudo-tethered ligand. *J Biol Chem* **272**(37):23186-23190.
- Moree WJ, Kataoka K, Ramirez-Weinhouse MM, Shiota T, Imai M, Tsutsumi T, Sudo M, Endo N, Muroga Y, Hada T, Fanning D, Saunders J, Kato Y, Myers PL and Tarby CM (2008) Potent antagonists of the CCR2b receptor. Part 3: SAR of the (R)-3-aminopyrrolidine series. *Bioorg Med Chem Lett* **18**(6):1869-1873.

MOL#86850

- Nicholls DJ, Tomkinson NP, Wiley KE, Brammall A, Bowers L, Grahames C, Gaw A, Meghani P, Shelton P, Wright TJ and Mallinder PR (2008) Identification of a putative intracellular allosteric antagonist binding-site in the CXC chemokine receptors 1 and 2. *Mol Pharmacol* **74**(5):1193-1202.
- Pease JE, Wang J, Ponath PD and Murphy PM (1998) The N-terminal extracellular segments of the chemokine receptors CCR1 and CCR3 are determinants for MIP-1alpha and eotaxin binding, respectively, but a second domain is essential for efficient receptor activation. *J Biol Chem* **273**(32):19972-19976.
- Quinones MP, Estrada CA, Kalkonde Y, Ahuja SK, Kuziel WA, Mack M and Ahuja SS (2005) The complex role of the chemokine receptor CCR2 in collagen-induced arthritis: implications for therapeutic targeting of CCR2 in rheumatoid arthritis. *J Mol Med (Berl)* **83**(9):672-681.
- Rosenkilde MM and Schwartz TW (2006) GluVII:06--a highly conserved and selective anchor point for non-peptide ligands in chemokine receptors. *Curr Top Med Chem* **6**(13):1319-1333.
- Salchow K, Bond ME, Evans SC, Press NJ, Charlton SJ, Hunt PA and Bradley ME (2010) A common intracellular allosteric binding site for antagonists of the CXCR2 receptor. *Br J Pharmacol* **159**(7):1429-1439.
- Samson M, LaRosa G, Libert F, Painsavoine P, Detheux M, Vassart G and Parmentier M (1997) The second extracellular loop of CCR5 is the major determinant of ligand specificity. *J Biol Chem* **272**(40):24934-24941.
- Scholten DJ, Canals M, Maussang D, Roumen L, Smit MJ, Wijtmans M, de Graaf C, Vischer HF and Leurs R (2011) Pharmacological modulation of chemokine receptor function. *Br J Pharmacol* **165**(6):1617-1643.
- Shin N, Baribaud F, Wang K, Yang G, Wynn R, Covington MB, Feldman P, Gallagher KB, Leffert LM, Lo YY, Wang A, Xue CB, Newton RC and Scherle PA (2009) Pharmacological characterization of INCB3344, a small molecule antagonist of human CCR2. *Biochem Biophys Res Commun* **387**(2):251-255.
- Smith PK, Krohn RI, Hermanson GT, Mallia AK, Gartner FH, Provenzano MD, Fujimoto EK, Goeke NM, Olson BJ and Klenk DC (1985) Measurement of protein using bicinchoninic acid. *Anal Biochem* **150**(1):76-85.
- Sohy D, Parmentier M and Springael JY (2007) Allosteric transinhibition by specific antagonists in CCR2/CXCR4 heterodimers. *J Biol Chem* **282**(41):30062-30069.
- Springael JY, Le Minh PN, Urizar E, Costagliola S, Vassart G and Parmentier M (2006) Allosteric modulation of binding properties between units of chemokine receptor homo- and hetero-oligomers. *Mol Pharmacol* **69**(5):1652-1661.
- Struthers M and Pasternak A (2010) CCR2 antagonists. *Curr Top Med Chem* **10**(13):1278-1298.
- Surgand JS, Rodrigo J, Kellenberger E and Rognan D (2006) A chemogenomic analysis of the transmembrane binding cavity of human G-protein-coupled receptors. *Proteins* **62**(2):509-538.
- Vauquelin G, Van Liefde I, Birzbier BB and Vanderheyden PM (2002) New insights in insurmountable antagonism. *Fundam Clin Pharmacol* **16**(4):263-272.
- White FA, Bhangoo SK and Miller RJ (2005) Chemokines: integrators of pain and inflammation. *Nat Rev Drug Discov* **4**(10):834-844.

MOL#86850

- Xi B, Yu N, Wang X, Xu X and Abassi YA (2008) The application of cell-based label-free technology in drug discovery. *Biotechnol J* **3**(4):484-495.
- Xue C MB, Feng H, Cao G, Huang T, Zheng C, Robinson DJ, Han A (2004) 3-Aminopyrrolidine derivatives as modulators of chemokine receptors. .
- Yu N, Atienza JM, Bernard J, Blanc S, Zhu J, Wang X, Xu X and Abassi YA (2006) Real-time monitoring of morphological changes in living cells by electronic cell sensor arrays: an approach to study G protein-coupled receptors. *Anal Chem* **78**(1):35-43.
- Zou D, Zhai HX, Eckman J, Higgins P, Gillard M, Knerr L, Carre S, Pasau P, Collart P, Grassi J, Libertine L, Nicolas JM and Schwartz CE (2007) Novel, acidic CCR2 receptor antagonists: from hit to lead. *Letters in Drug Design & Discovery* **4**:185-191.

MOL#86850

Footnotes

This study was performed and financially supported within the framework of Top
Institute Pharma, project number D1-301.

MOL#86850

Figure legends

Figure 1. Chemical structures of reference CCR2 small molecule antagonists.

Figure 2. Characterization of ^{125}I -CCL2 binding to membranes of U2OS cells stably expressing CCR2. (A) Homologous competition assay of 0.1 nM and 0.05 nM ^{125}I -CCL2 in presence of increasing concentrations of unlabeled CCL2. Non specific binding was determined in presence of 10 μM INCB3344. (B) Association and dissociation kinetics of 0.1 nM ^{125}I -CCL2 binding to CCR2 at 37°C. Dissociation was initiated by the addition of 10 μM INCB3344. Association and dissociation rate constants were $0.29 \pm 0.06 \text{ nM}^{-1} \text{ min}^{-1}$ and $0.033 \pm 0.003 \text{ min}^{-1}$ respectively. Data was best fitted using a one-phase association and one-phase exponential decay function. For all experiments a representative graph of one experiment performed in duplicate is shown (see Table 1 for K_D , B_{max} values).

Figure 3. Displacement of (A) ^{125}I -CCL2 binding, (B) [^3H]-INCB3344 binding and (C) [^3H]-CCR2-RA binding to U2OS membranes stably expressing CCR2 by increasing concentrations of CCL2 and six reference CCR2 antagonists. Results are presented as percentage of bound radioligand for one representative experiment performed in duplicate (see Table 2 for affinity values).

Figure 4. Characterization of [^3H]-INCB3344 binding to membranes of U2OS cells stably expressing CCR2. (A) Saturation binding of [^3H]-INCB3344 to CCR2. Different concentrations of [^3H]-INCB3344 were incubated in presence (non-specific binding) or

MOL#86850

absence (total binding) of 10 μM BMS22. Specific binding was determined by subtracting the non-specific binding from the total binding. (B) Association and dissociation kinetics of 1.8 nM [^3H]-INCB3344 to CCR2 at 25°C. Dissociation was initiated by the addition of 10 μM BMS22. Association and dissociation rate constants were $0.054 \pm 0.002 \text{ nM}^{-1} \text{ min}^{-1}$ and $0.013 \pm 0.002 \text{ min}^{-1}$ respectively. Data was best fitted using a one-phase association and one-phase exponential decay function. For all experiments a representative graph of one experiment performed in duplicate is shown (see Table 1 for K_D , B_{max} values).

Figure 5. Characterization of [^3H]-CCR2-RA binding to membranes of U2OS cells stably expressing CCR2. (A) Saturation binding of [^3H]-CCR2-RA to CCR2. Different concentrations of [^3H]-CCR2-RA were incubated in presence (non-specific binding) or absence (total binding) of 10 μM JNJ-27141491. Specific binding was determined by subtracting the non-specific binding from the total binding. (B) Association kinetics of 3 nM [^3H]-CCR2-RA to CCR2 at 25°C. Data was best fitted using a one-phase association function resulting in a k_{obs} of $0.089 \pm 0.005 \text{ min}^{-1}$. (C) Dissociation kinetics of 3 nM [^3H]-CCR2-RA to CCR2 at 25°C. Dissociation was initiated by the addition of 10 μM JNJ-27141491. Data was best fitted using a two-phase exponential decay function, resulting in a k_{off1} of $0.24 \pm 0.02 \text{ min}^{-1}$ and a k_{off2} of $0.029 \pm 0.005 \text{ min}^{-1}$. For all experiments a representative graph of one experiment performed in duplicate is shown (see Table 1 for K_D , B_{max} values).

MOL#86850

Figure 6. (A) CCL2-induced beta-arrestin recruitment to U2OS cells stably expressing CCR2. (B) Inhibition of CCL2-induced beta-arrestin recruitment to CCR2. Cells were incubated with a concentration of CCL2 that evoked 80% of the maximum response (5 nM). Increasing concentrations of the antagonists were added to determine their IC₅₀ value. For all experiments basal activity was set at 0% and the maximum response at 100%. Results are presented for one representative experiment performed in duplicate (see Table 3 for IC₅₀ values).

Figure 7. Impedance measurements in the xCELLigence label-free assay for U2OS cells stably expressing CCR2. (A) Representative graph of baseline-corrected normalized Cell Index (CI) after addition of different concentrations of CCL2. (B) Concentration-response curve for CCL2 derived from peak-height analysis of CI changes for the 5 min interval after application. (C) Inhibition of CCL2-induced impedance measurements. Cells were incubated with a concentration of CCL2 that evoked 80% of the maximum response (3 nM). Increasing concentrations of the antagonists were added 30 min before agonist stimulation to determine their IC₅₀ value, derived from peak-height analysis of CI changes for the 5 min interval after application of CCL2. Results are presented for one representative experiment performed in duplicate (see Table 3 for IC₅₀ values).

Figure 8. [³⁵S]-GTPγS binding to membranes of U2OS cells stably expressing CCR2. (A) Inhibition of CCL2-induced [³⁵S]-GTPγS binding by six small molecule antagonists. Membranes were incubated with a concentration of CCL2 that evoked 80% of the maximum response (10 nM). Increasing concentrations of the antagonists were added to

MOL#86850

determine their IC_{50} value. (B,C) Concentration-effect curves of CCL2-induced [^{35}S]-GTP γ S binding. Increasing concentrations of CCL2 were added simultaneously with indicated concentrations of INCB3344 (B) or CCR2-RA-[R] (C). For all experiments basal activity was set at 0% and the maximum response at 100%. Results are presented as mean percentage \pm S.E.M. of three experiments performed in duplicate (see Table 4 for pEC_{50} and E_{max} values).

MOL#86850

Tables

Table 1. Equilibrium binding parameters of ^{125}I -CCL2, [^3H]-INCB3344 and [^3H]-CCR2-RA, determined on U2OS membranes expressing CCR2.

	^{125}I -CCL2	[^3H]-INCB3344	[^3H]-CCR2-RA
K_D (nM)	0.068 ± 0.014^a	0.90 ± 0.03^b	5.8 ± 0.2^c
B_{\max} (pmol/mg)	0.31 ± 0.03^a	7.1 ± 0.2^b	9.7 ± 0.2^c

Data are presented as mean \pm S.E.M. of three experiments performed in duplicate.

^aHomologous displacement of ^{125}I -CCL2 from CCR2 at 37°C.

^bSaturation binding of 0.5 - 45 nM [^3H]-INCB3344 to CCR2 at 25°C.

^cSaturation binding of 0.2 - 75 nM [^3H]-CCR2-RA to CCR2 at 25°C.

MOL#86850

Table 2. Displacement of ^{125}I -CCL2, [^3H]-INCB3344 and [^3H]-CCR2-RA from U2OS membranes expressing CCR2.

Compound	^{125}I -CCL2	[^3H]-INCB3344	[^3H]-CCR2-RA
	displacement $\text{IC}_{50} \pm \text{S.E.M. (nM)}$	displacement $\text{K}_i \pm \text{S.E.M. (nM)}$ or % binding	displacement $\text{K}_i \pm \text{S.E.M. (nM)}$ or % binding
CCL2	0.19 ± 0.04	$79 \pm 2\%^a$	$77 \pm 4\%^a$
INCB3344	5.4 ± 0.8	1.2 ± 0.1	$169 \pm 17\%^{b*}$
BMS22	27 ± 4	5.1 ± 1.3	$164 \pm 16\%^{b*}$
RS504393	132 ± 25	62 ± 3	$157 \pm 16\%^{b*}$
Teijin	220 ± 26	107 ± 10	$159 \pm 17\%^{b*}$
JNJ-27141491	172 ± 15	$112 \pm 3\%^{b*}$	12 ± 3
CCR2-RA-[R]	103 ± 18	$109 \pm 1\%^{b*}$	5.0 ± 0.8

Data are presented as mean \pm S.E.M. of at least three experiments performed in duplicate.

^a Percentage of radioligand binding in presence of 100 nM CCL2. 100% was determined in the presence of buffer and therefore values < 100% represent displacement.

^b Percentage of radioligand binding in presence of 1 μM antagonist. 100% was determined in the presence of buffer and therefore values >100% represent enhancement

* $p < 0.05$, Student's t-test.

MOL#86850

Table 3. Inhibition of CCL2 induced cellular responses measured in [³⁵S]-GTPγS membrane binding assays as well as beta-arrestin recruitment and xCELLigence label free whole cell assays.

Compound	³⁵ S]-GTPγS	Beta-arrestin	xCELLigence ^a
	binding inhibition	recruitment	IC ₅₀ ± S.E.M.
	IC ₅₀ ± S.E.M. (nM)	inhibition IC ₅₀ ± S.E.M. (nM)	(nM)
INCB3344	2.8 ± 0.8	3.2 ± 0.2	2.0 ± 0.5
BMS22	5.5 ± 1.8	4.8 ± 0.4	21 ± 6*
RS504393	19 ± 7**	68 ± 3	87 ± 15
Teijin	183 ± 48	67 ± 13	292 ± 66*
JNJ-27141491	3.9 ± 1.0**	29 ± 1	25 ± 4
CCR2-RA-[R]	24 ± 3	25 ± 4	64 ± 14***

Data are presented as mean ± S.E.M. of three experiments performed in duplicate.

^aInhibition of CCL2 was calculated from concentration-response curves derived from peak-analysis of CI changes.

*p<0.05, vs. beta-arrestin data; ANOVA, Tukey's MCT.

**p<0.05, vs. beta-arrestin and xCELLigence data; ANOVA, Tukey's MCT.

***p<0.05, vs. [³⁵S]-GTPγS and beta-arrestin data; ANOVA, Tukey's MCT.

MOL#86850

Table 4. G protein activation by CCL2 measured by [³⁵S]-GTPγS binding. Potency and maximum effect of CCL2 in the absence or presence of different concentrations of CCR2-RA-[R].

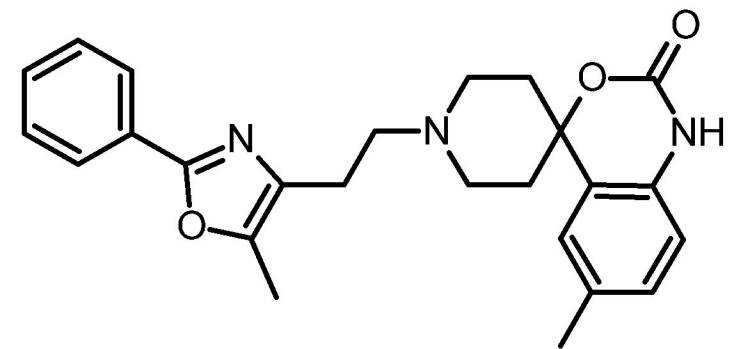
	pEC₅₀ ± S.E.M.	E_{max} ± S.E.M. (%)
control	8.3 ± 0.1	104 ± 4
+ 1 nM INCB3344	7.6 ± 0.1*	103 ± 7
+ 3 nM INCB3344	7.0 ± 0.3*	102 ± 14
+ 10 nM INCB3344	6.2 ± 0.9	ND ^a
+ 10 nM CCR2-RA-[R]	7.7 ± 0.1*	81 ± 6 ^{**}
+ 30 nM CCR2-RA-[R]	7.7 ± 0.1*	55 ± 4 ^{***}
+ 100 nM CCR2-RA-[R]	7.6 ± 0.1*	30 ± 3 ^{***}

^aNot determined.

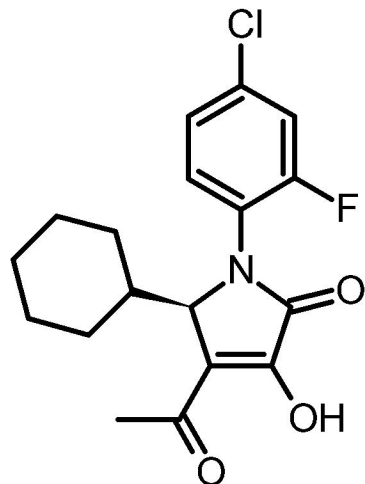
Data are presented as mean ± S.E.M. of at least three experiments (*p<0.05, ** p< 0.001,

*** p< 0.0001 vs. control, Student's t-test)

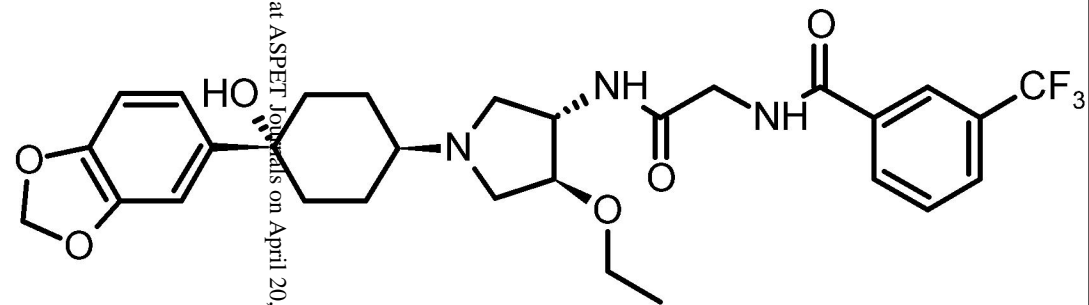
Figure 1



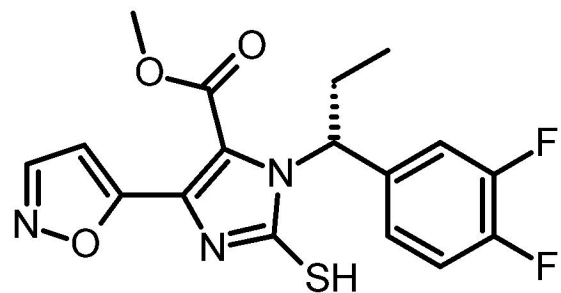
RS504393



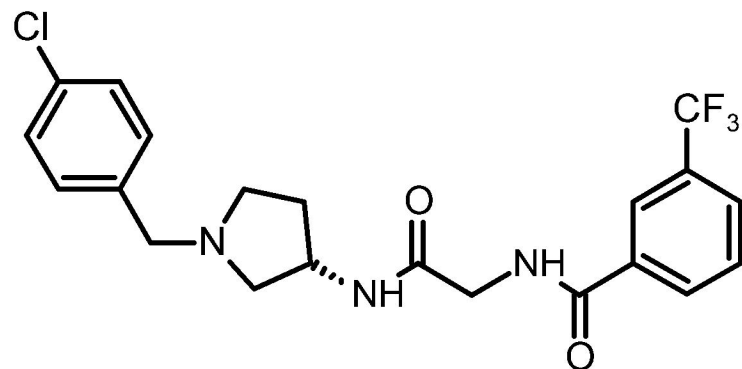
CCR2-RA-[R]



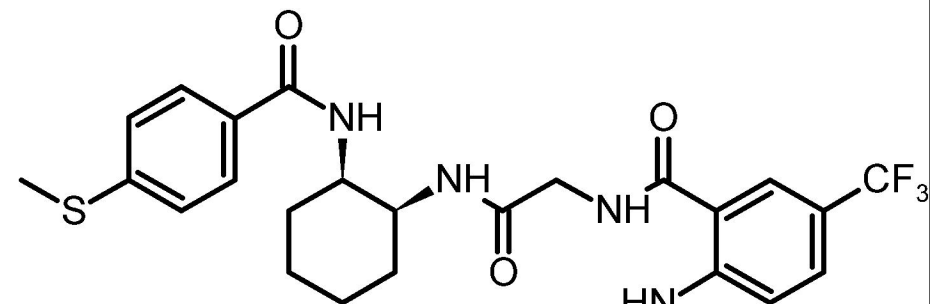
INCB3344



JNJ-27141491



Teijin



BMS22

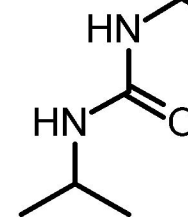


Figure 2

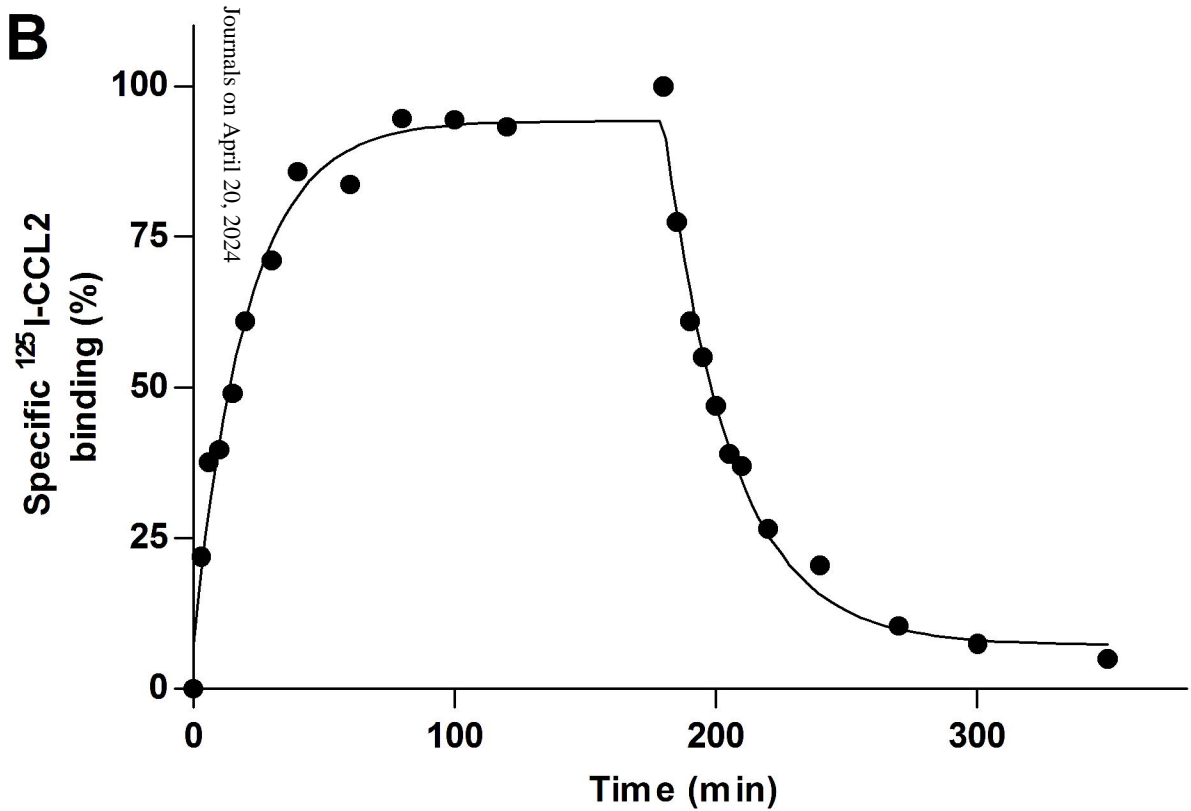
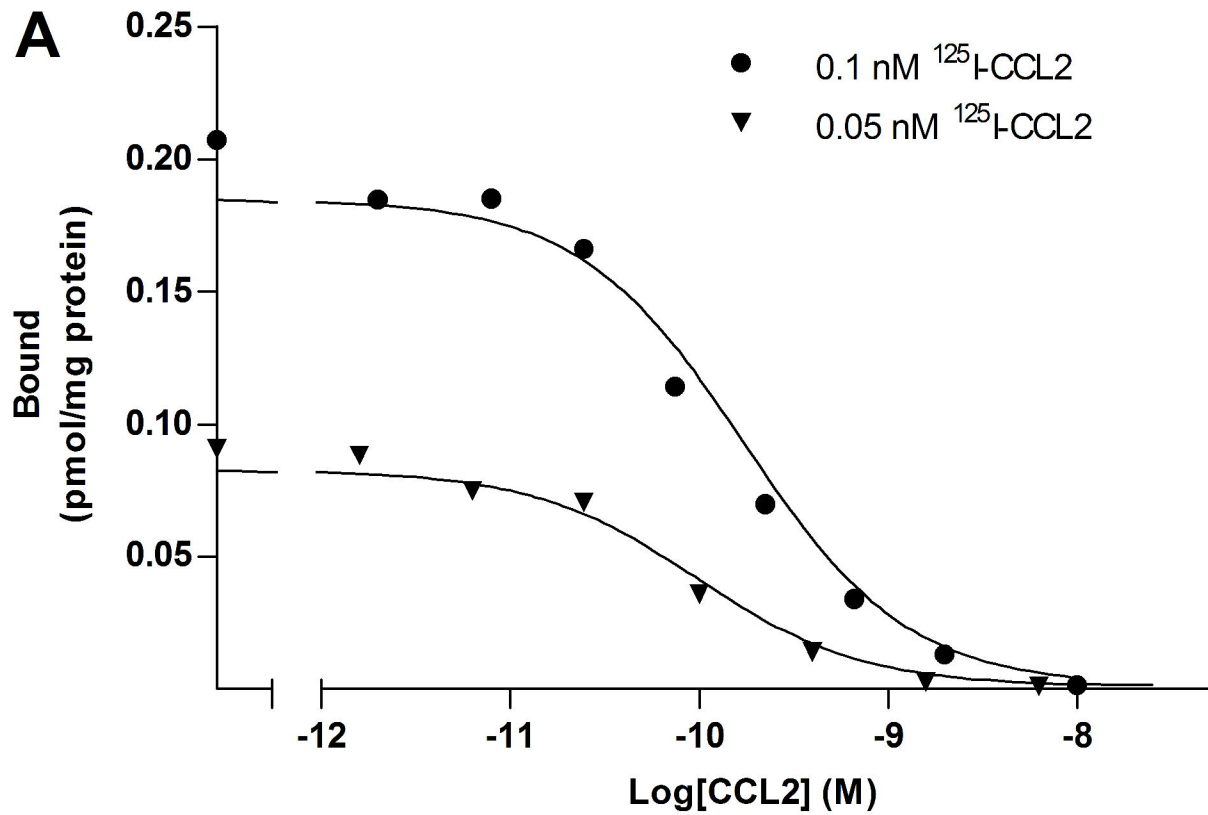


Figure 3

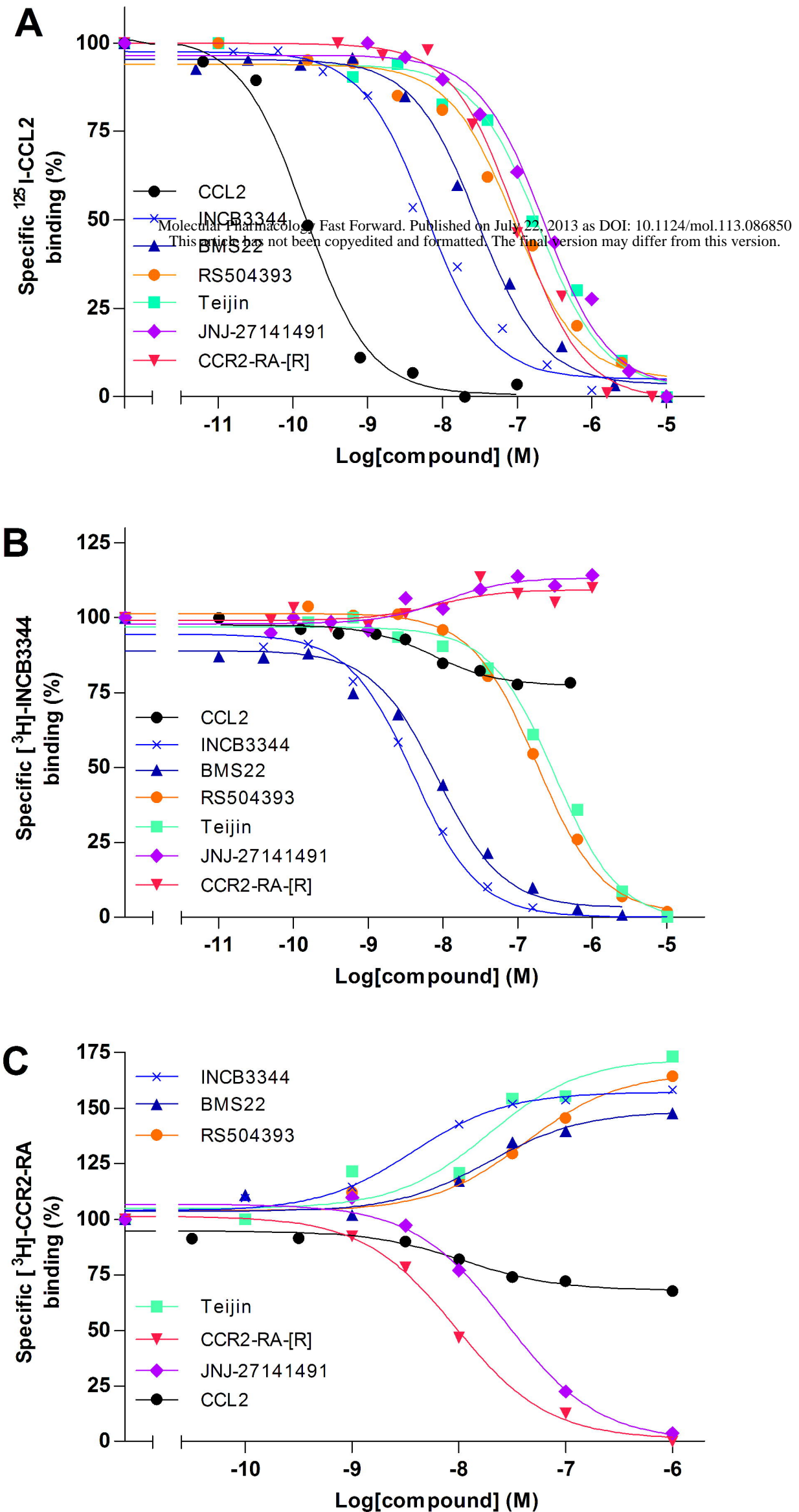


Figure 4

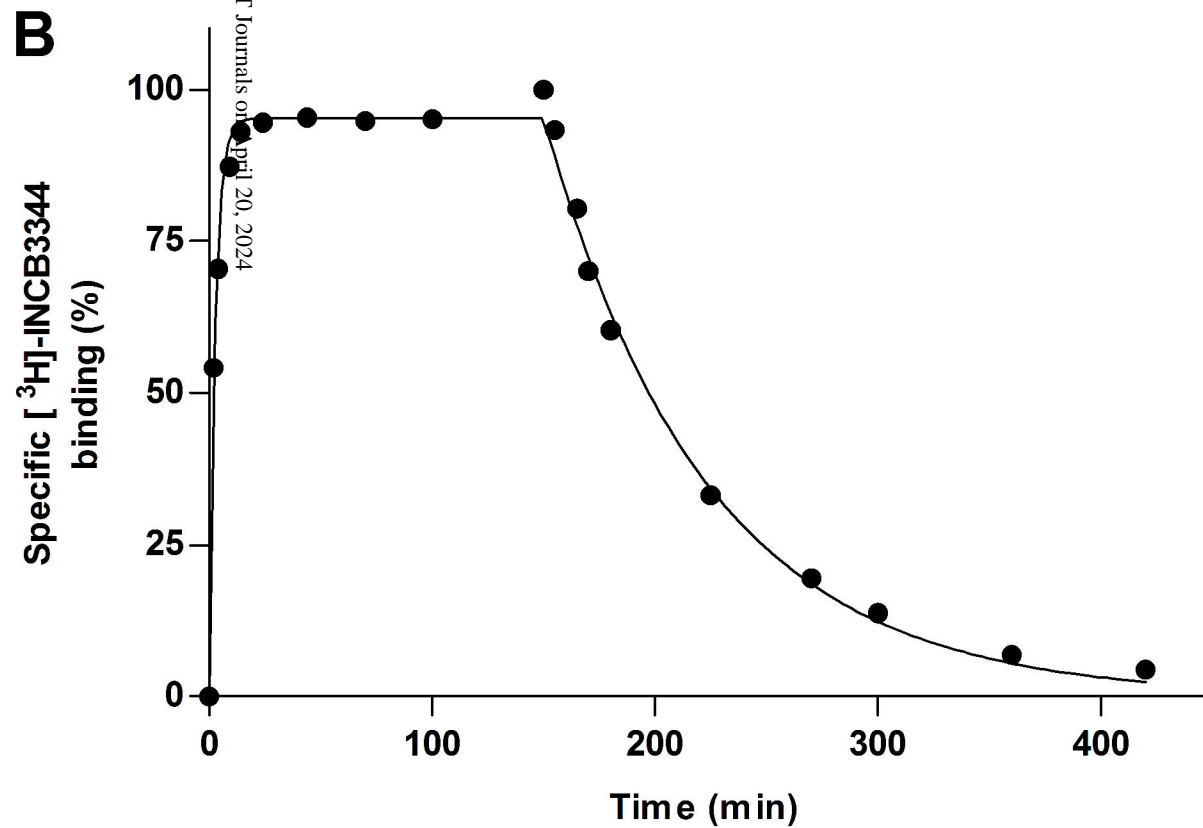
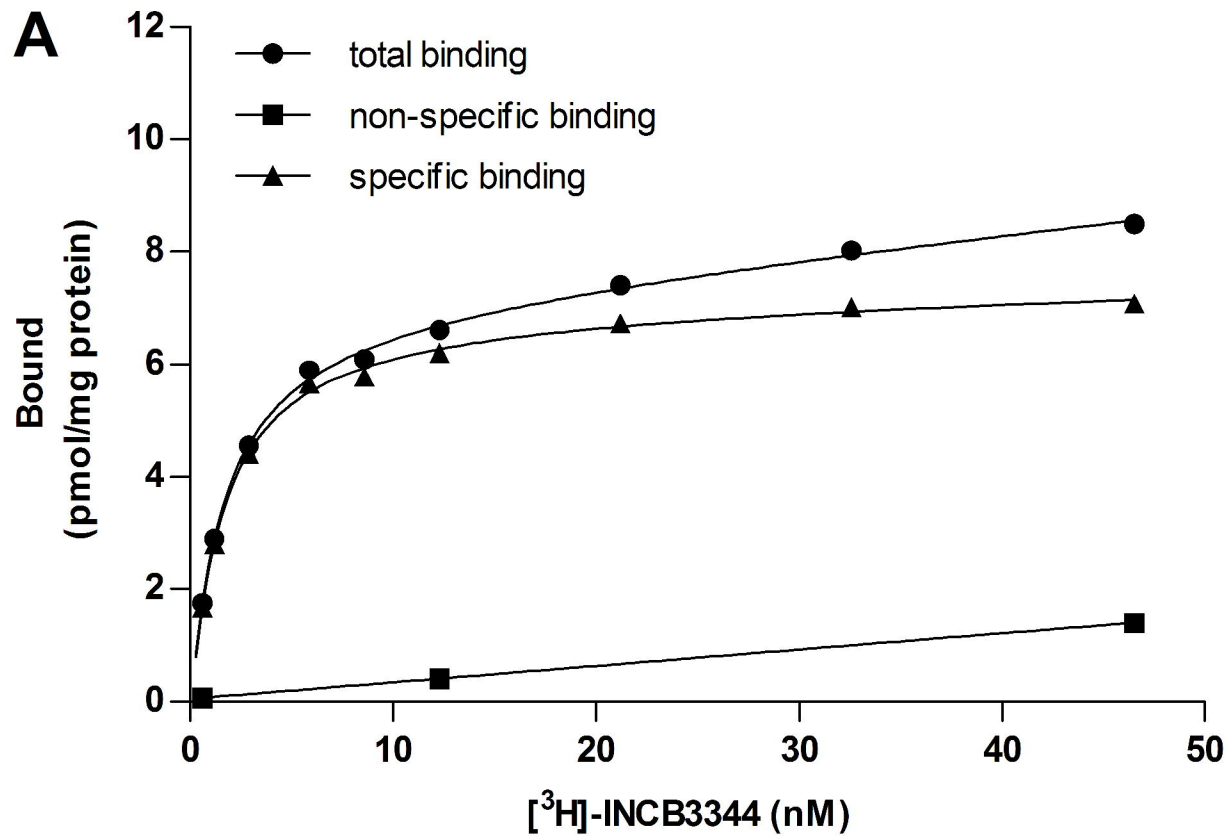


Figure 5

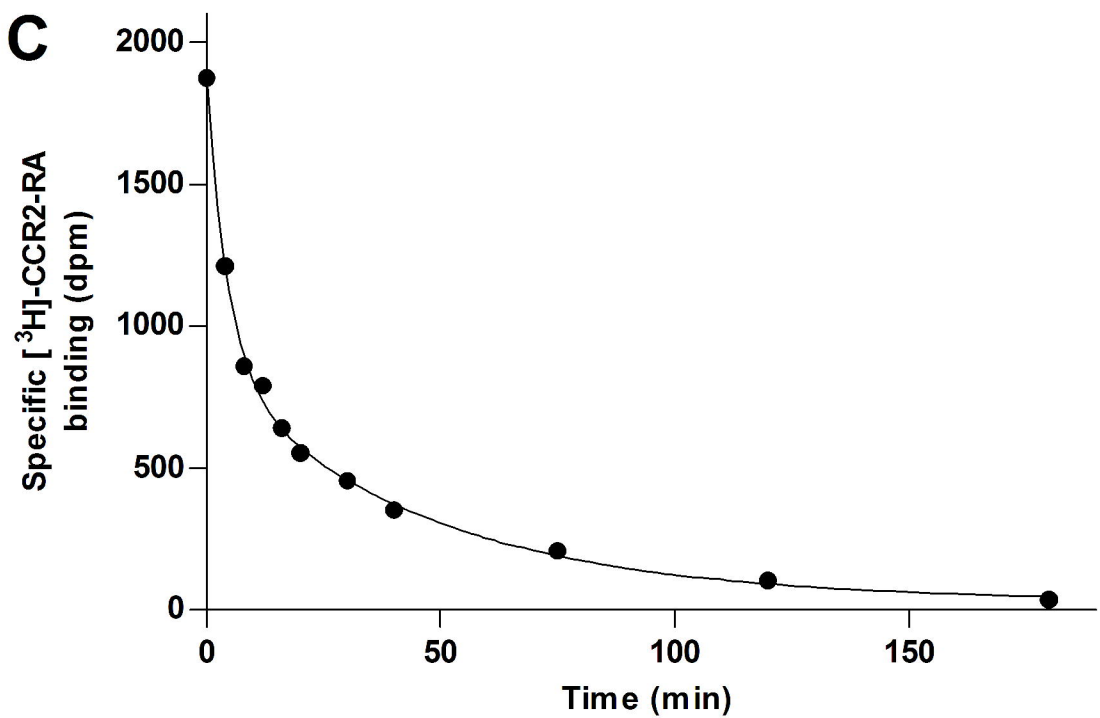
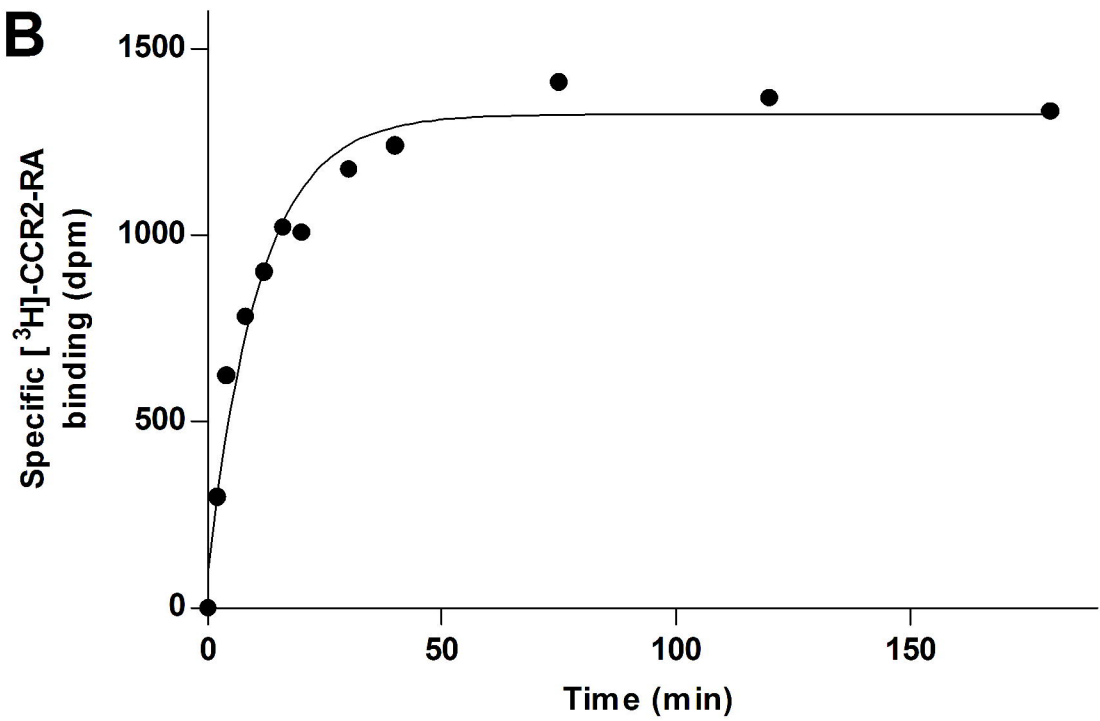
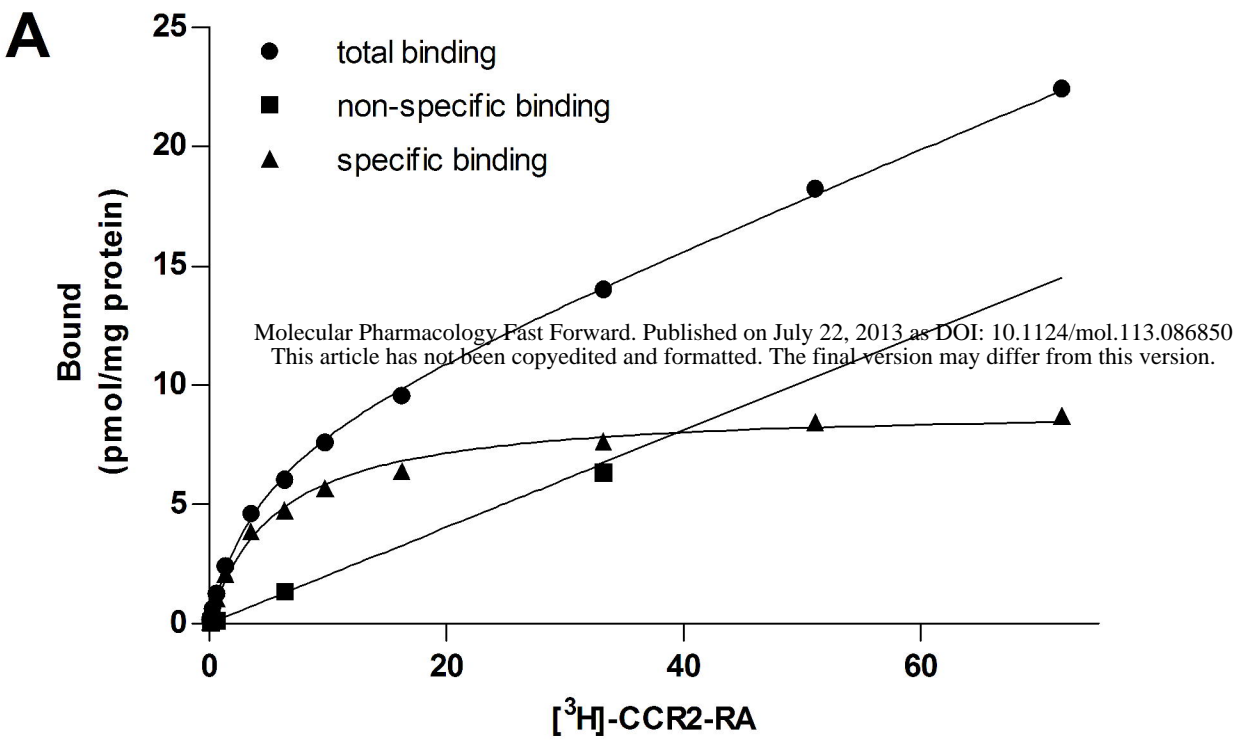


Figure 6

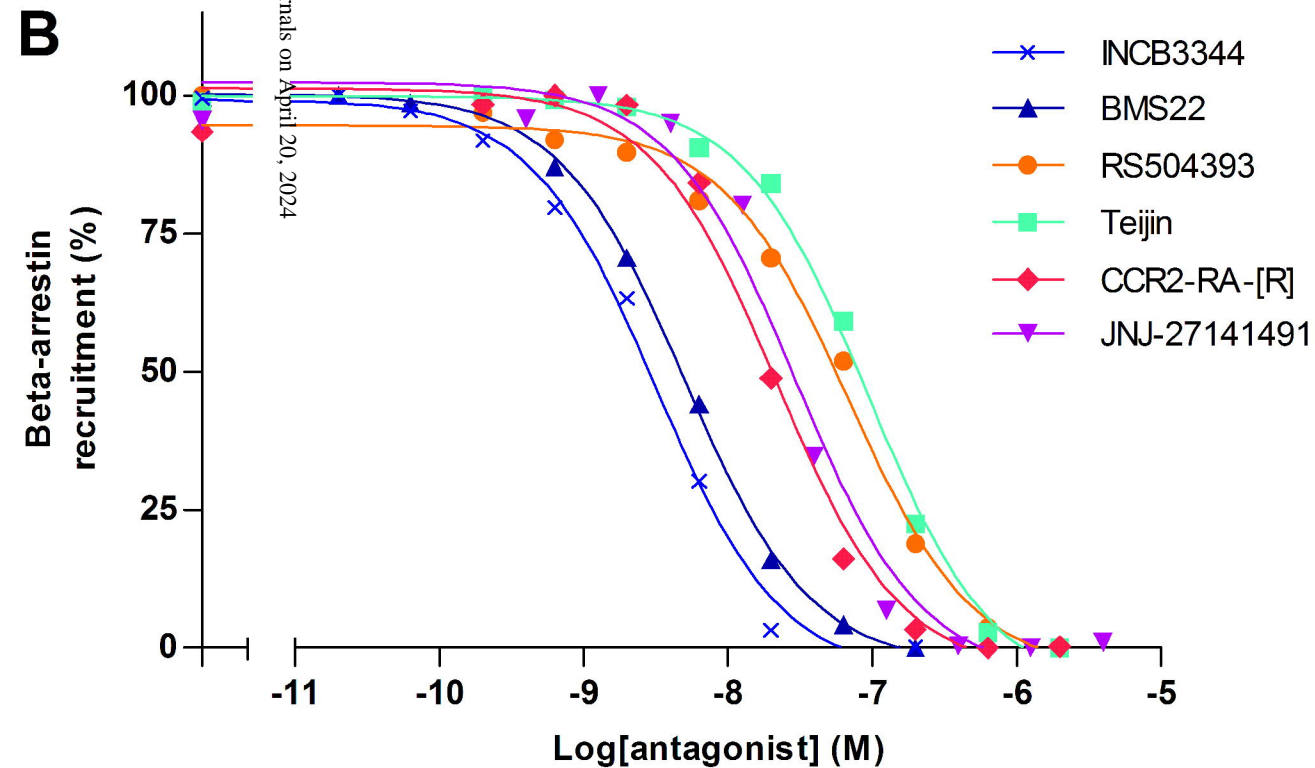
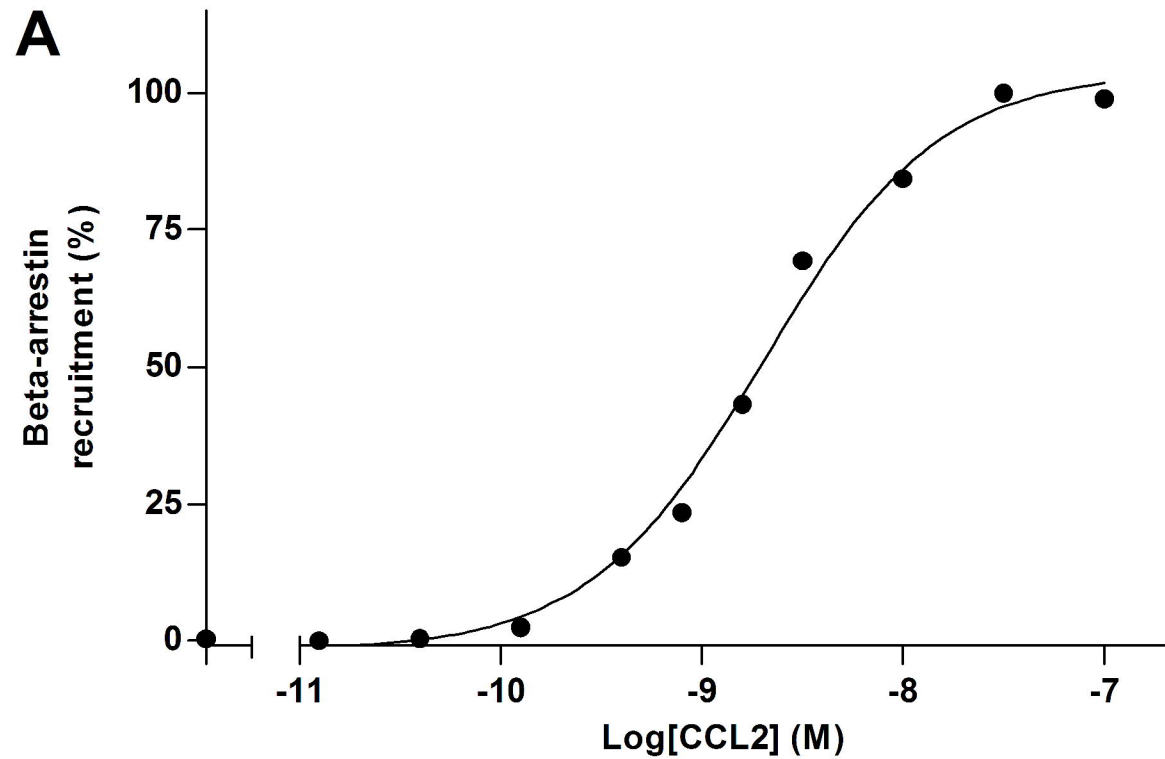


Figure 7

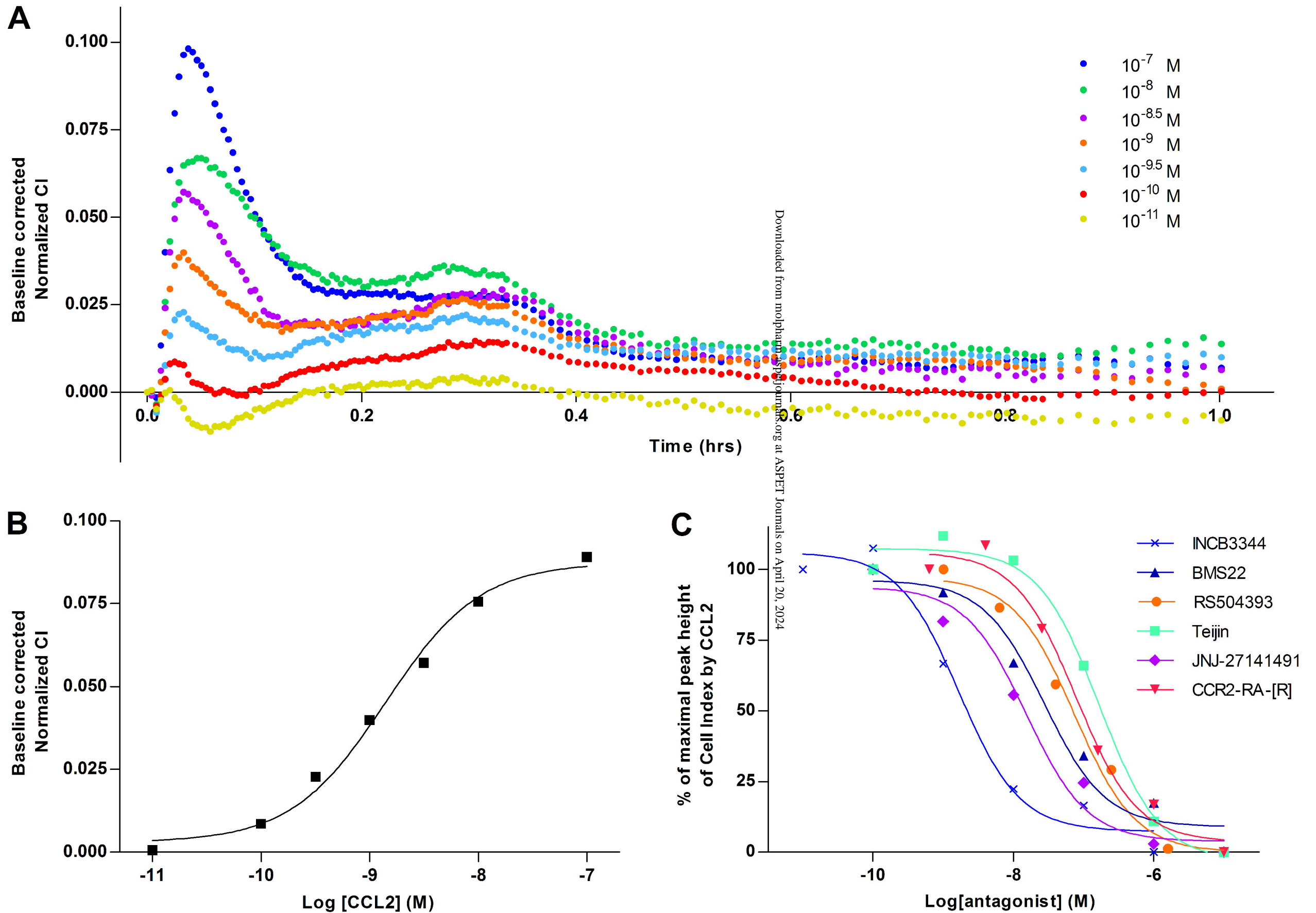
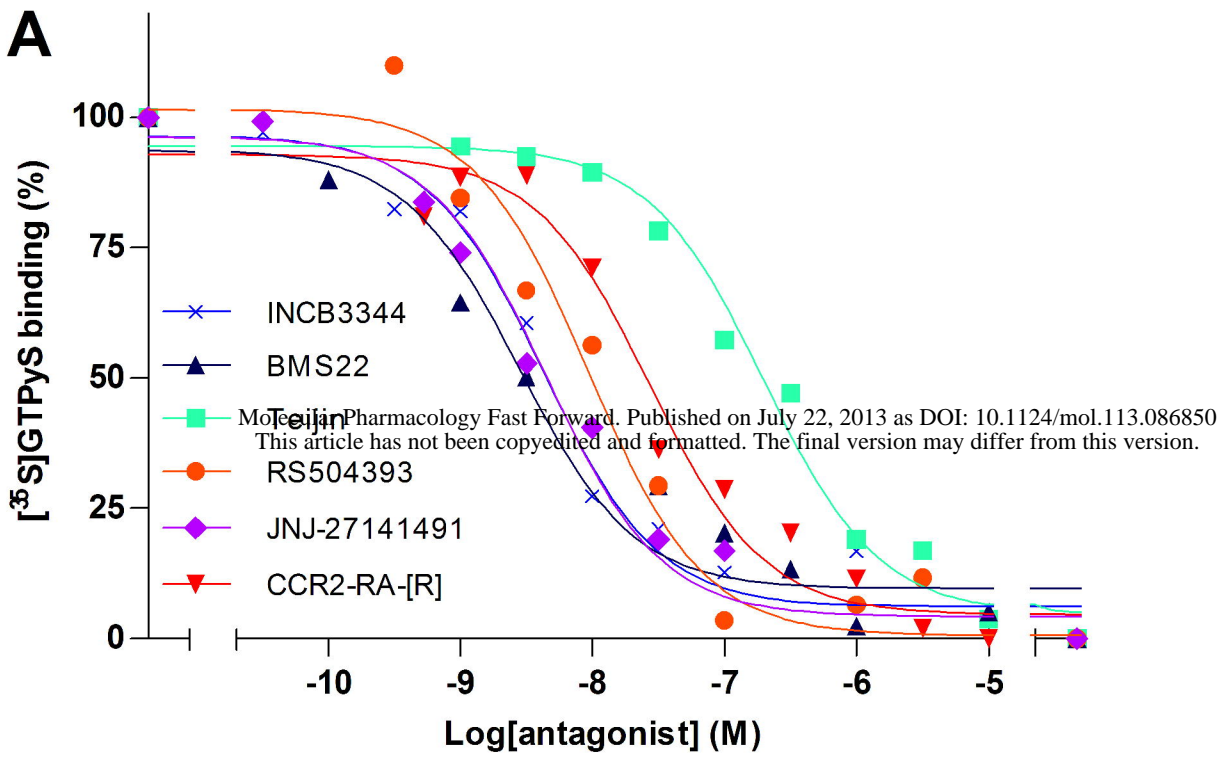
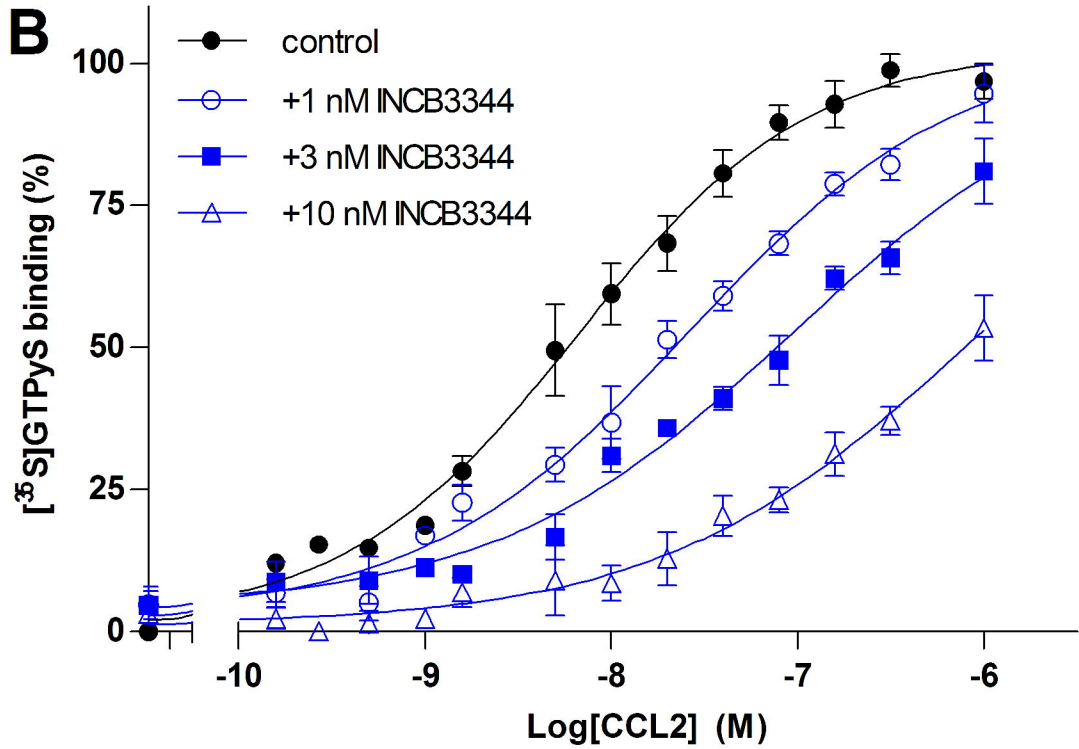


Figure 8

A



B



C

